POLYTECHNIC UNIVERSITY OF CATALONIA
BARCELONATECH
Terrassa School of Industrial, Aerospace and Audiovisual Engineering

Master in Aerospace Engineering

Esther Mas Sanz

Origin and mineralogy of Lunar meteorites. A study for lunar mining and resources exploitation

Master's Final Degree Project - **Annexes**

Director: Dr. Josep M. Trigo-Rodríguez (CSIC-IEEC)

Tutor: Dr. Miquel Sureda Anfres (UPC)

Course: 2019-2020, Spring Semester

Delivery date: 22^{nd} June, 2020

[This page intentionally left blank]

Contents

List of Figures

List of Tables

A. Annexes

A.1 Orbital Dynamics

This section explains the different reference frames and coordinate systems used during the project.

A.1.1 Randomly distributed points on the lunar surface

A set of N points are randomly distributed on the Moon's surface. These points are the origin launch sites for the lunar ejecta which can be launched at an specific **local elevation** and **local azimuth** given a velocity.

The process followed has been:

- **Generation of the launch site subespace:** given a point on the surface of the Moon P, a vector $\hat{w}$ is defined as $\hat{w} = \overrightarrow{OP}/||\overrightarrow{OP}||$, where O is the centre of an spherical Moon. The $\hat{w}$ vector defines the direction of the local vertical. If $\hat{k}$ is defined as the global vertical direction ($\hat{k} = [0, 0, 1]$), then $\hat{w}$ and $\hat{k}$ define a plane that slices the Moon in an arbitrary meridian. Then, $\hat{w} \times \hat{k} = \overrightarrow{u}$, $\hat{u} = \overrightarrow{u}/||\overrightarrow{u}||$ being $\hat{u}$ orthonormal to the aforementioned plane and to $\hat{w}$ and $\hat{k}$. The $\hat{u}$ vector is considered to be the local direction pointing towards west. Eventually, $\hat{w} \times \hat{u} = \hat{v}$, being $\hat{v}$ orthonormal to $\hat{w}$ and $\hat{u}$ and pointing to the local south direction. The three vectors $< \hat{u}, \hat{v}, \hat{v} >$ form an orthonormal base, which is the local base used in the launching site.

- **Construction of the velocity director vector:** there are two inputs that the user has introduced previously, the elevation ϕ that goes from $[0, \pi/2]$ and its origin is set at the local vertical $\hat{w}$. The local azimuth θ has its origin set at $\hat{u}$ and takes values from $[02\pi]$ always being contained in the plane defined by $\hat{u}$ and $\hat{v}$. The modulus of the velocity is V and the velocity vector in the base $< \hat{u}, \hat{v}, \hat{v} >$ is defined as:

$$V_u = V \sin\phi \cos\theta$$
$$V_v = V \sin\phi \sin\theta$$
$$V_w = V \cos\phi$$

  Finally, the velocity vector in the local base $\overrightarrow{V}_{uvw}$ must be transformed to the global one $\overrightarrow{V}_{ijk}$ being: $\overrightarrow{V}_{ijk} = \mathbf{T}\overrightarrow{V}_{uvw}$, where T is the transformation matrix formed by

the base vectors themselves:

$$T = \begin{bmatrix} u_1 & v_1 & w_1 \\ u_2 & v_2 & w_2 \\ u_3 & v_3 & w_3 \end{bmatrix}$$

- **Change of reference frame:** once each launching site has its velocity vector assigned, vectors (velocity and position) must be expressed in the chosen reference frame of the HORIZONS ephemeris data [2], ICFR/J2000. In order to do that the following transformations are made:

$$\overrightarrow{r}_{LaunchSite/Sun} = \overrightarrow{r}_{LaunchSite/Moon} + \overrightarrow{r}_{Moon/Sun}$$
$$\overrightarrow{v}_{LaunchSite/Sun} = \overrightarrow{v}_{LaunchSite/Moon} + \overrightarrow{v}_{Moon/Sun}$$

  For the second transformation, one velocity term is **missing**, the one that takes into account the additional velocity of the particles for being at a non-inertial surface of the Moon (as it rotates) $\overrightarrow{V}_{MoonSurface} = \overrightarrow{\Omega} \times \overrightarrow{R}_{Moon}$ (with $\overrightarrow{\Omega}$ the lunar rotational velocity and $\overrightarrow{R}_{Moon}$ the radius of the Moon). This term has been considered negligible[1].

A.1.2 Lunar coordinate system and Lunar Maps

In this work there are several representations of the geography of the Moon, mainly being maps with topographical coordinates indicating the latitude and longitude of the location. Lunar geographical maps, as terrestrial ones, obey a convention to establish the direction of the cardinal directions. The reader is referred to [3] for a detailed review on different types of lunar coordinates to be used in astronomy.

For this project the criteria has been the following:

- The Moon coordinate system is *mooncentric*, meaning that the Moon is assumed to be a perfect sphere. From its centre, an orthonormal base is defined.
- A parallelism is established with *geocentric* coordinates: the vertical axis will be defined by the axis of rotation of the Moon and will define the lunar North Pole. A perpendicular plane to the North vector and containing the centre of the Moon-sphere will divide the Moon in two halves, defining the Moon equator.
- Considering that the axial tilt of the Moon is 1º32' from the ecliptic [1], the North direction axis of the Moon can be considered parallel to the normal direction to the

[1] The Moon rotates in its own axis taking roughly ≈ 28 days. Hence $\Omega = \frac{2\pi}{T} = \frac{2\pi}{28d \cdot 24h \cdot 60min \cdot 60sec} = 2.6 \cdot 10^{-6}\, s^{-1}$. The radius is $R_{Moon} = 1737.1km$, then $\overrightarrow{\Omega} \times \overrightarrow{R}_{Moon} = 4.5 \cdot 10^{-3} km/s$. A velocity of barely $4.5m/s$ compared to the escape velocity of $2.38km/s$ can be neglected.

ecliptic plane. The lunar north direction vector will be defined as $\hat{z}_M$.

- The East direction vector $\hat{y}_M$ is defined as the normal vector of the plane formed by $\hat{z}_M$ and $\overrightarrow{ME}$ (a unitary vector in the direction from the *mooncentric* origin to the *geocentric* origin), $\hat{y}_M = \hat{z}_M \times \overrightarrow{ME}$. To complete the orthonormal base, $\hat{x}_M = \hat{y}_M \times \hat{z}_M$. Vectors $\hat{x}_M$ and $\hat{y}_M$ will be contained in the ecliptic plane, by definition.

The base $< \hat{x}_M, \hat{y}_M, \hat{z}_M >$ is in turn the transformation matrix that particles will undergo from the ICFR/J2000 base to the *mooncentric* base. In particular, due to the approximation of the lunar north pole axis to the normal direction of the ecliptic the transformation from ICFR/J2000 to *mooncentric* coordinates will only consist of a rotation around the $\hat{z}_M$ axis that will vary as a function of the relative position of the Earth and the Moon.

A.2 Additional Tests

During the study of the parameters that influence the fate of lunar ejecta, it is paramount to ensure that results are not a particular case but a general one to yield solid conclusions. The main tests have been run with a population of $N = 500$ lunar ejecta and the rest (tests to verify results) with a population of $N = 300$ to speed up computing time.

A.2.1 Variation of the launch direction

Here are provided more plots of the launch angle vs. time for particular cases not included in the main text.

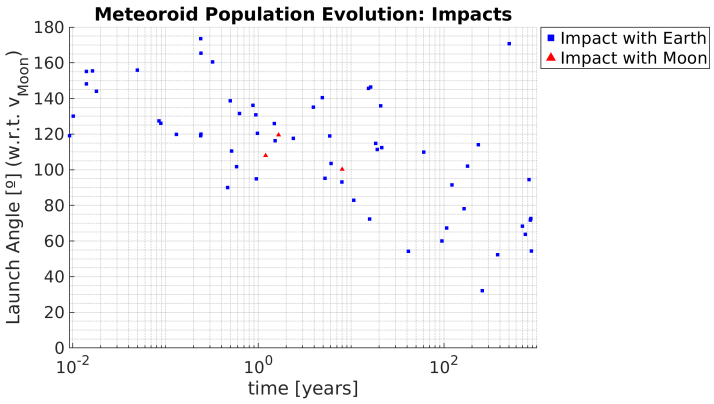

(a) Launch towards North at 2.6 km/s

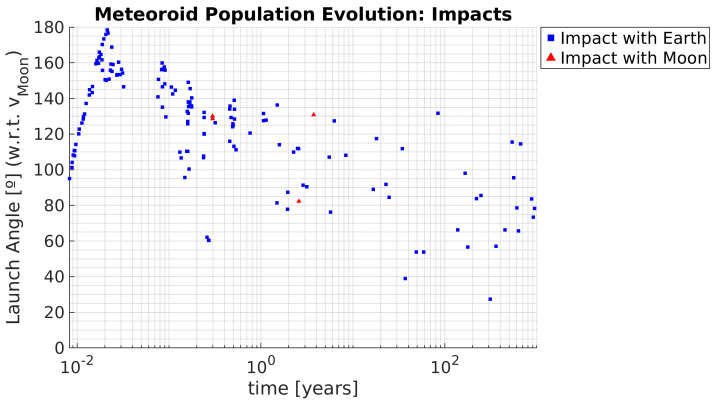

(b) Launch towards East at 2.6 km/s

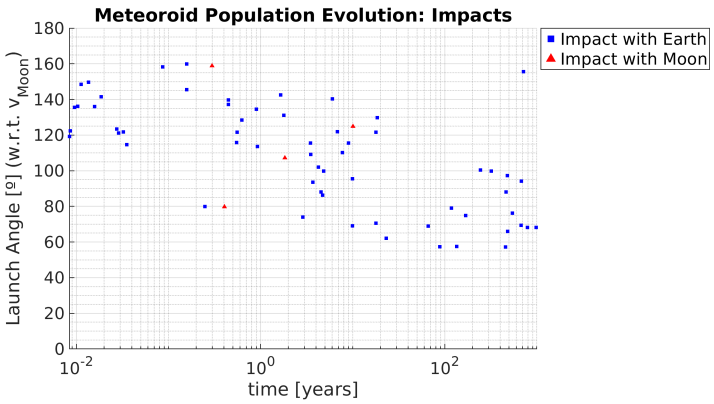

(c) Launch towards South at 2.6 km/s

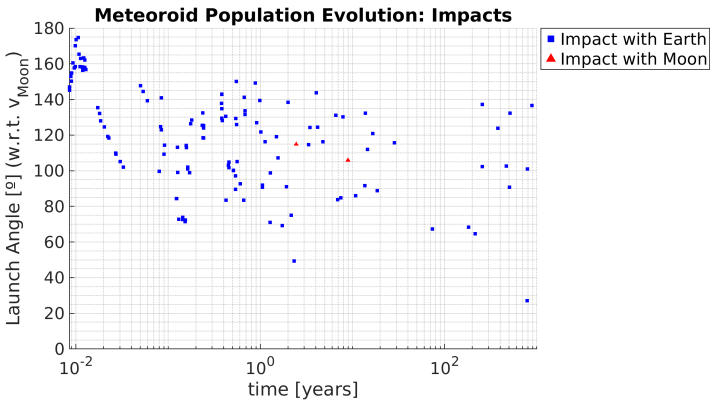

(d) Launch towards West at 2.6 km/s

Figure A.1: Evolution of the meteoroid impact population (logarithmic scale) for velocity 2.6km/s for the four different local directions of the launch.

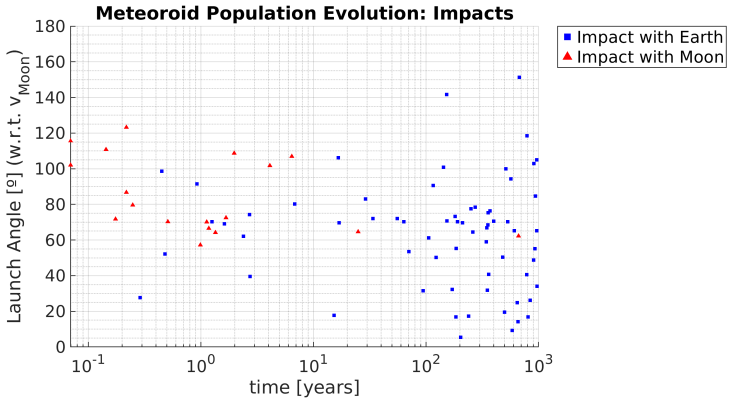

(a) Launch towards North at 2.4 km/s

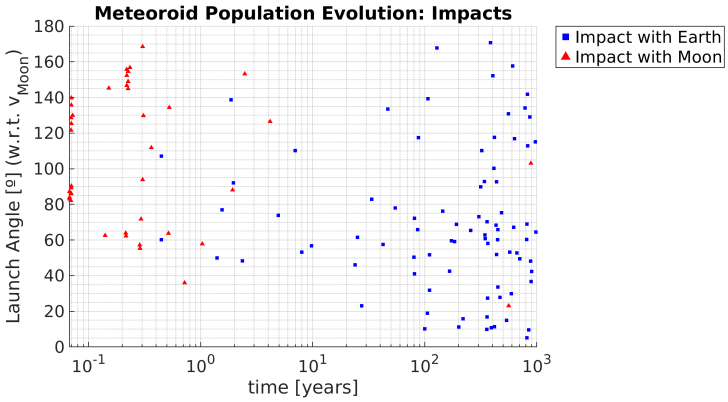

(b) Launch towards East at 2.4 km/s

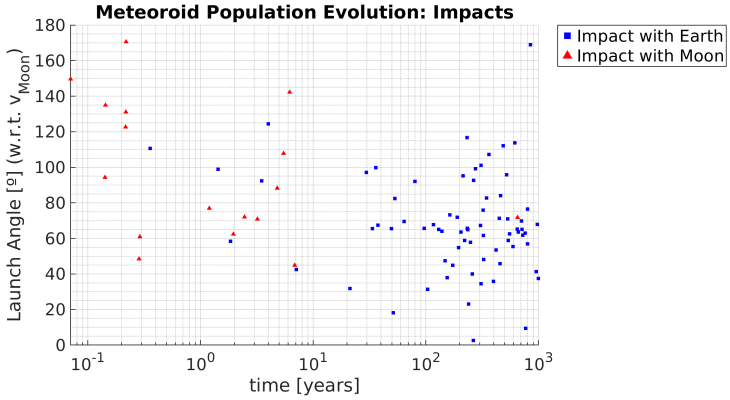

(c) Launch towards South at 2.4 km/s

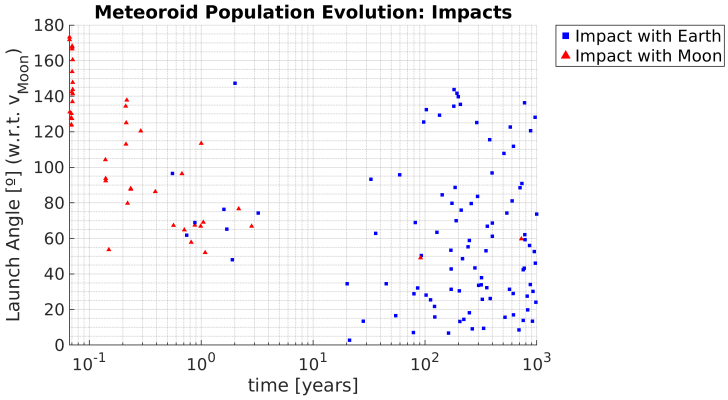

(d) Launch towards West at 2.4 km/s

Figure A.2: Evolution of the meteoroid impact population (logarithmic scale) for velocity 2.4km/s for the four different local directions of the launch.

A.2.2 Variation of ejection angle

The tests carried out for the Section 5.1.1 (Variation of the launch direction) were also performed when varying the ejection angle to verify the previous conclusions held. As results complied with the previous conclusions it has not been considered relevant to include them in the section. The reader can find here additional graphs that support the claims in Section 5.1.2.

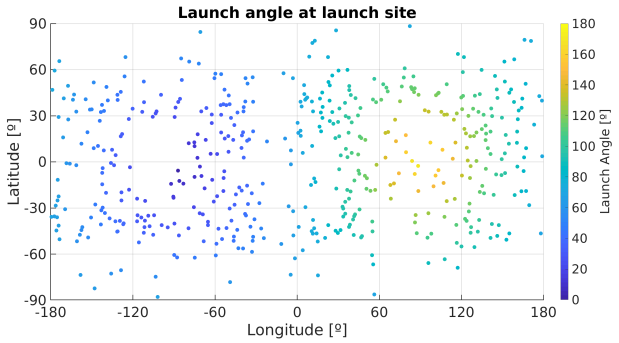

(a) Launch towards North

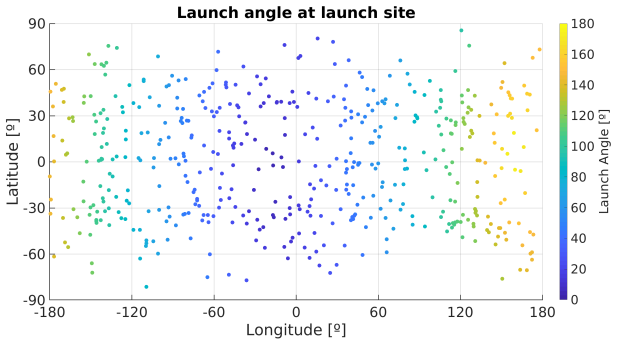

(b) Launch towards East

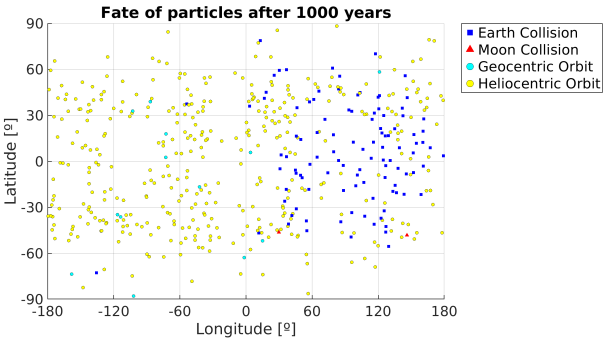

(c) Launch towards North

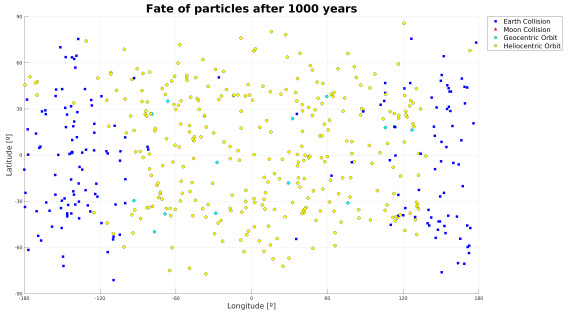

(d) Launch towards East

Figure A.3: Launch angle and particle's fate according to their launch site for different ejection angles.

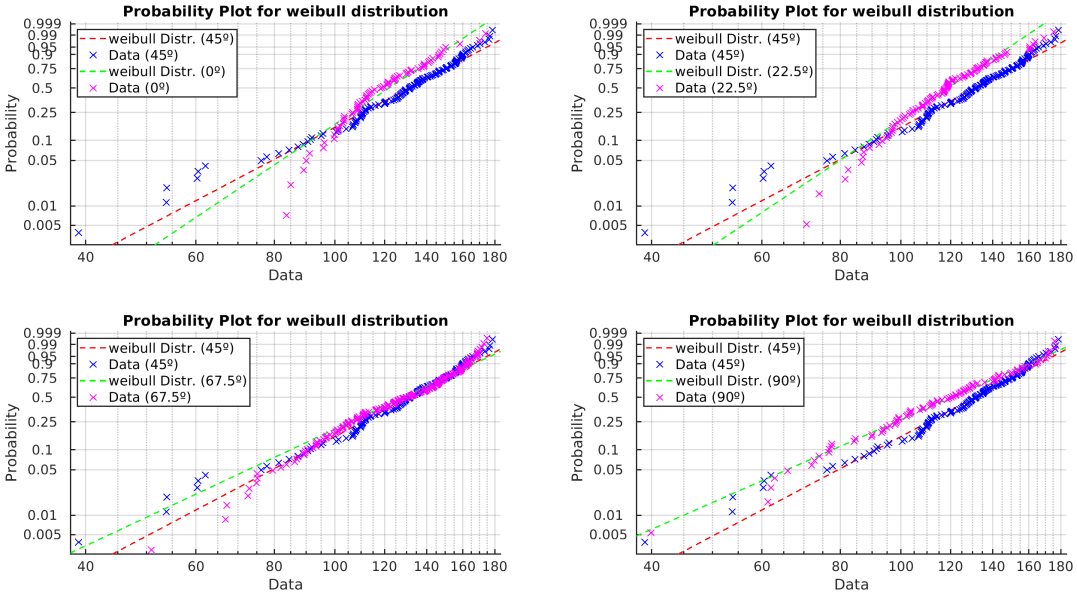

(a) Launch at 2.6km/s towards the East

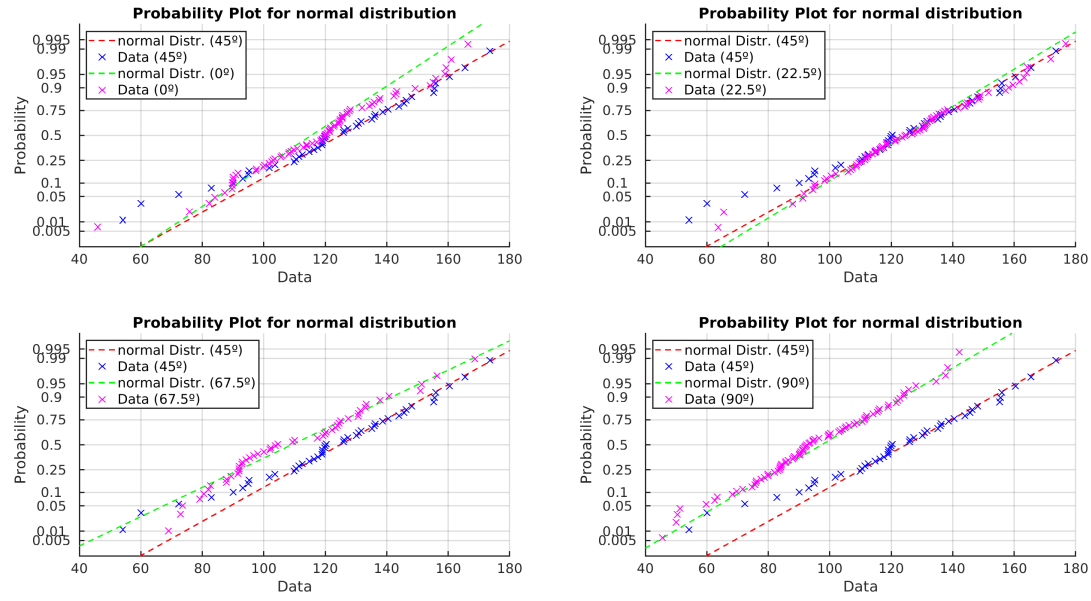

(b) Launch at 2.6 km/s towards the North

Figure A.4: Probability distribution of data.

A.2.3 Variation of E-M-S configuration

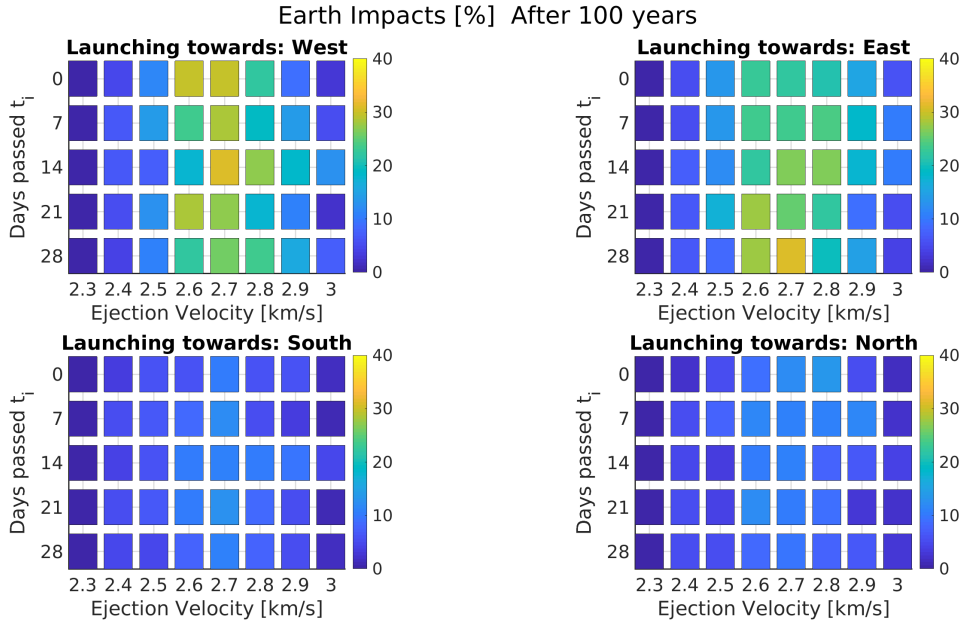

Figure A.5: Earth impacts for different velocities and initial dates. Additional test #1 of 300 particles.

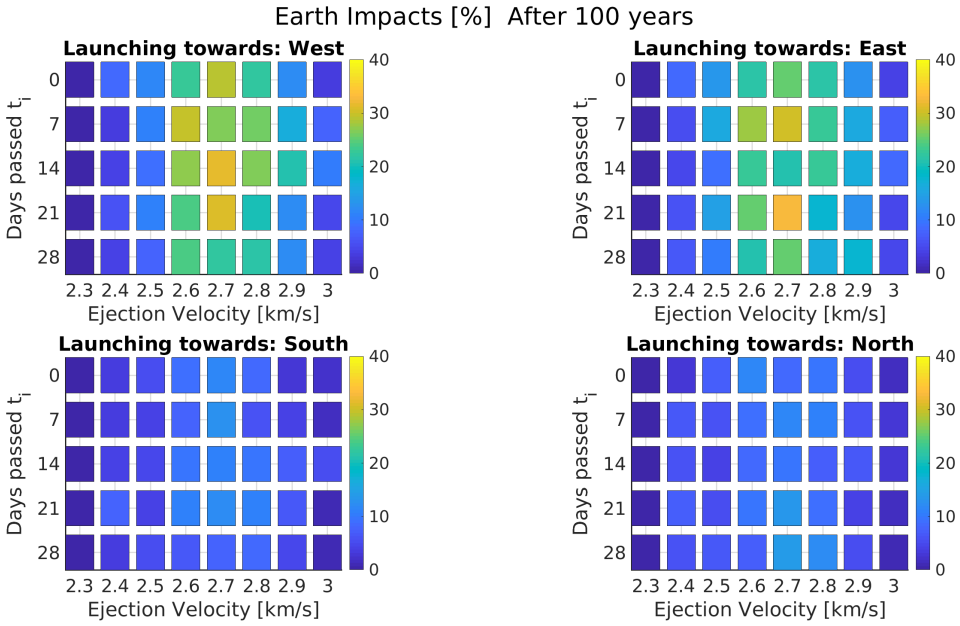

Figure A.6: Earth impacts for different velocities and initial dates. Additional test #2 of 300 particles.

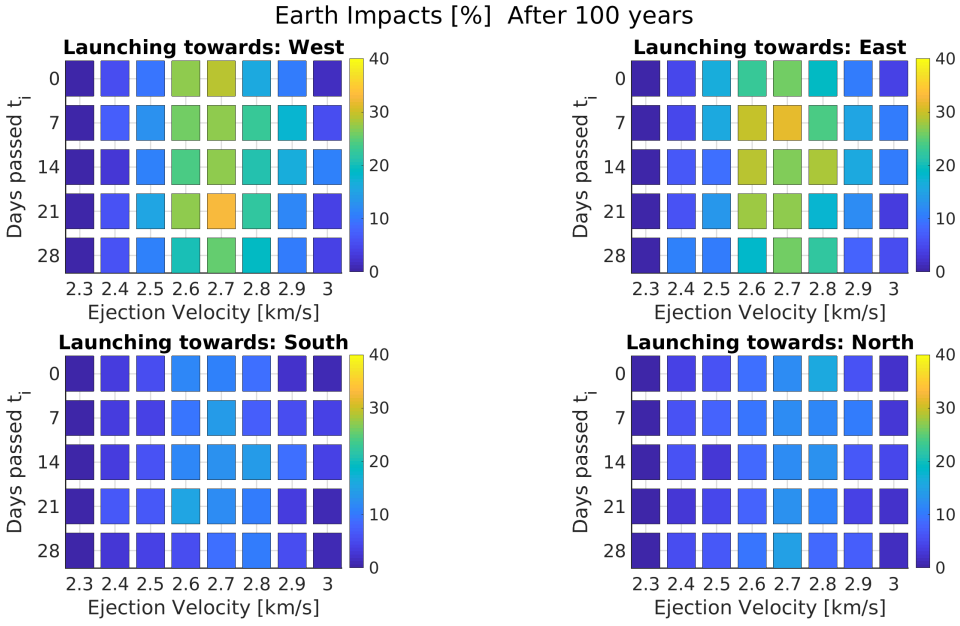

Figure A.7: Earth impacts for different velocities and initial dates. Additional test #3 of 300 particles.

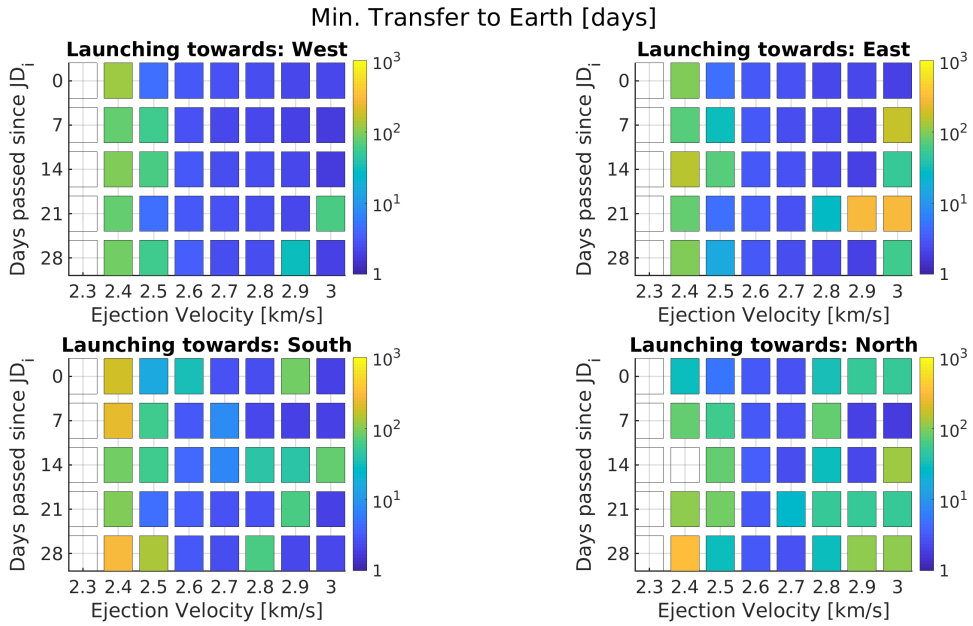

Figure A.8: Minimum time for a lunar ejecta to impact with Earth, in days. Additional test #1 of 300 particles.

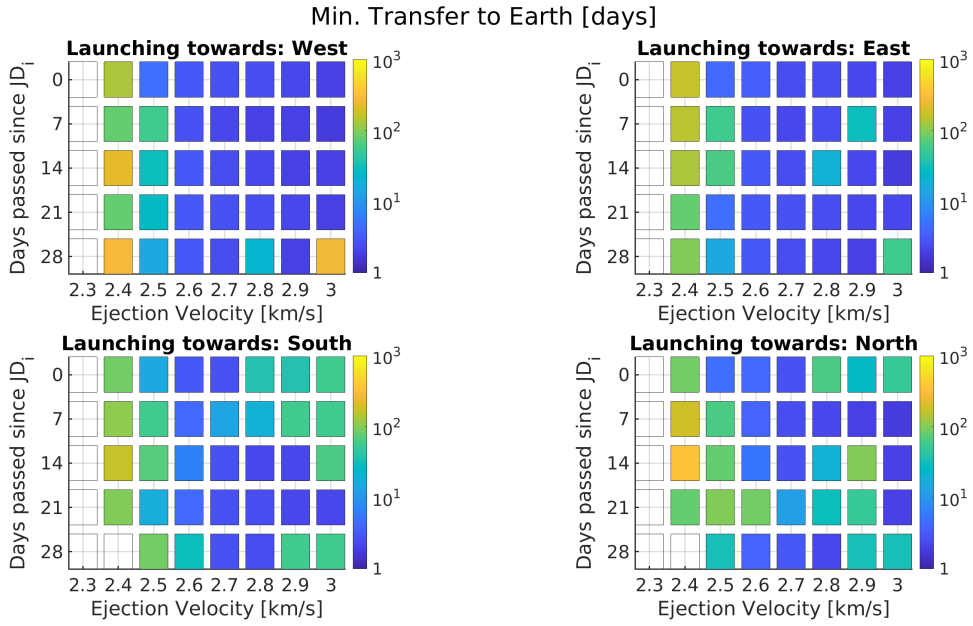

Figure A.9: Minimum time for a lunar ejecta to impact with Earth, in days. Additional test #2 of 300 particles.

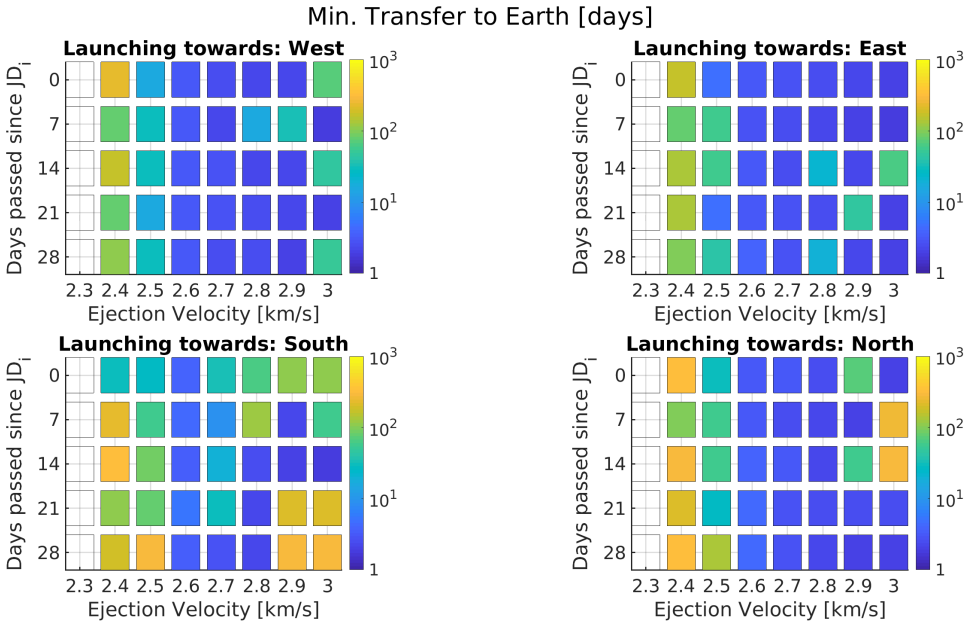

Figure A.10: Minimum time for a lunar ejecta to impact with Earth, in days. Additional test #3 of 300 particles.

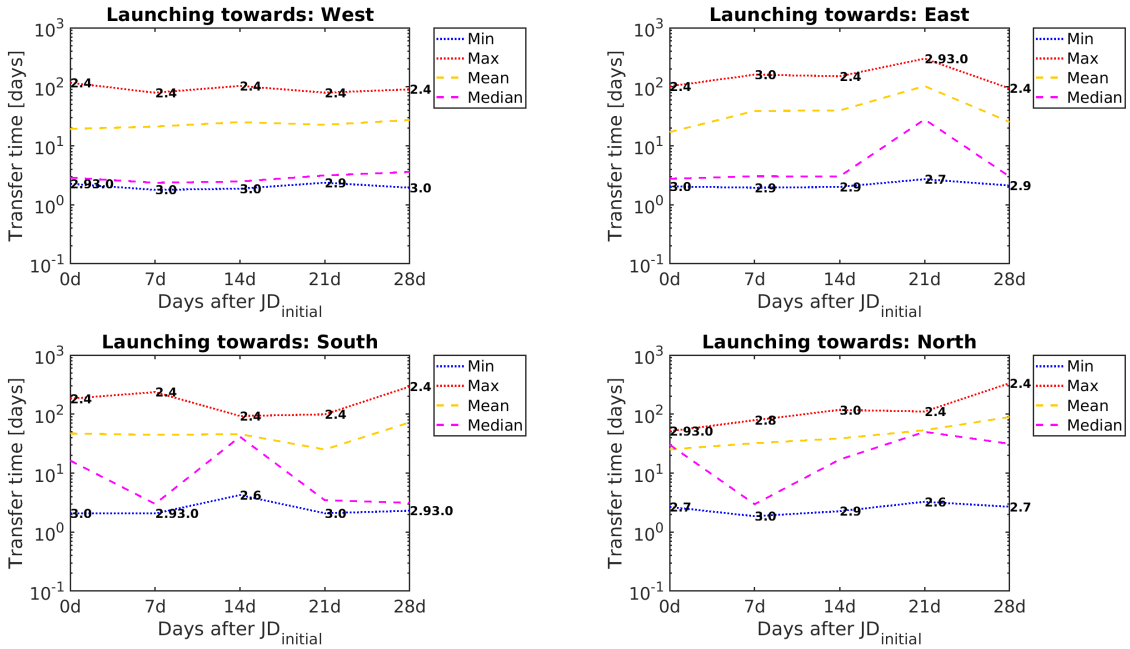

Figure A.11: Characteristic times for a lunar ejecta to impact with Earth. Additional test #1 of 300 particles.

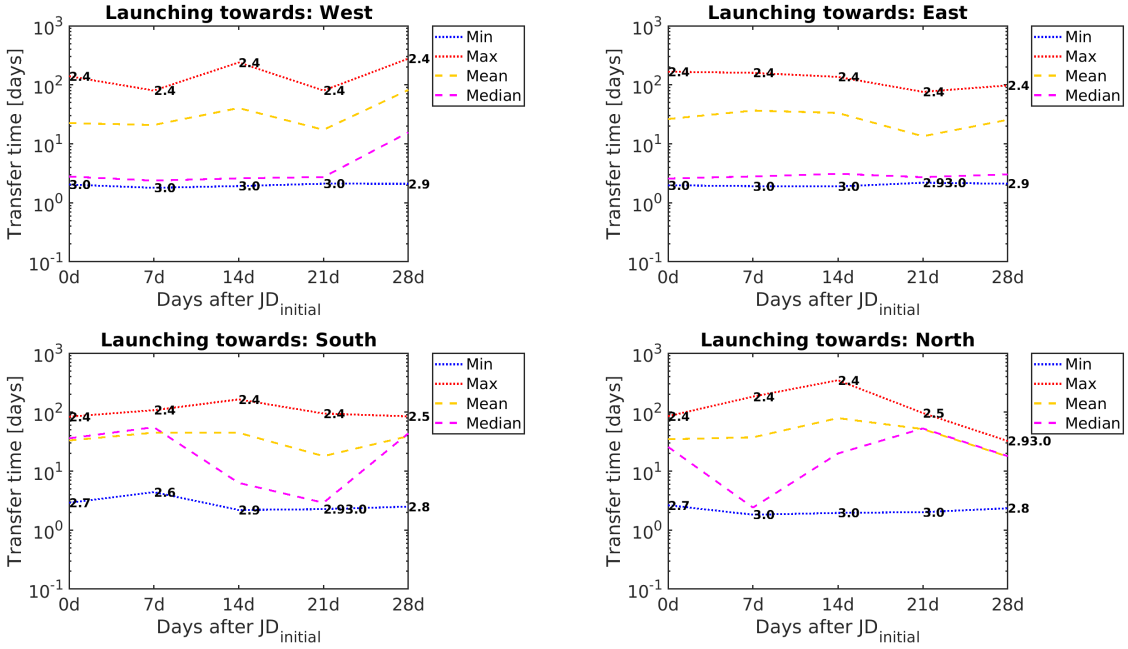

Figure A.12: Characteristic times for a lunar ejecta to impact with Earth. Additional test #2 of 300 particles.

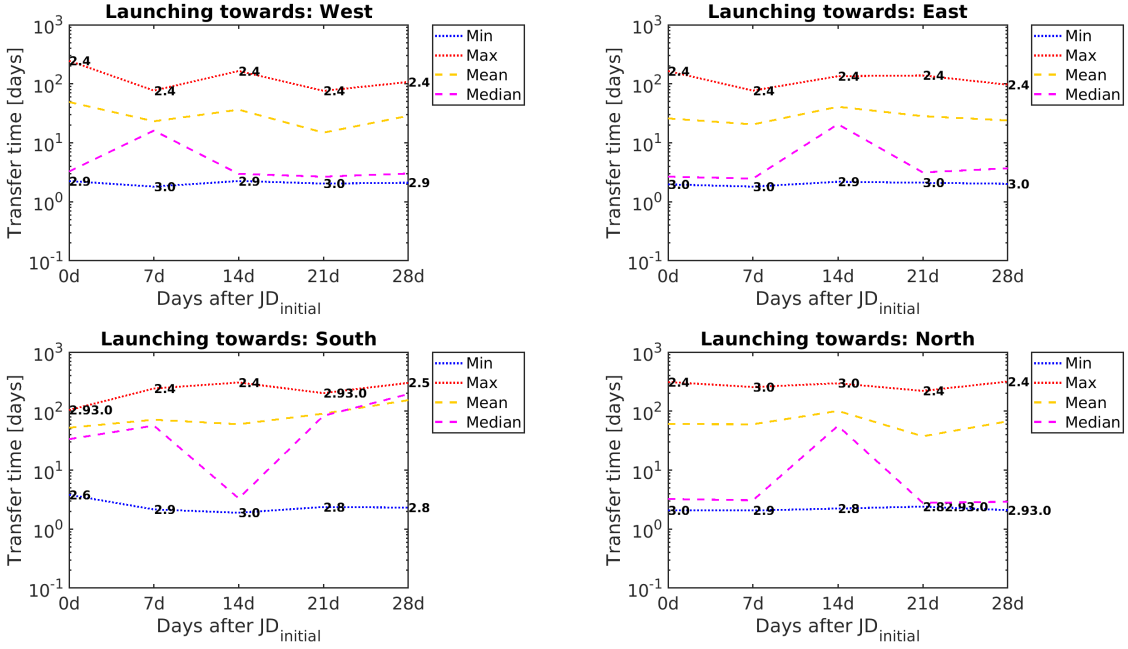

Figure A.13: Characteristic times for a lunar ejecta to impact with Earth. Additional test #3 of 300 particles.

A.2.4 Long transfers

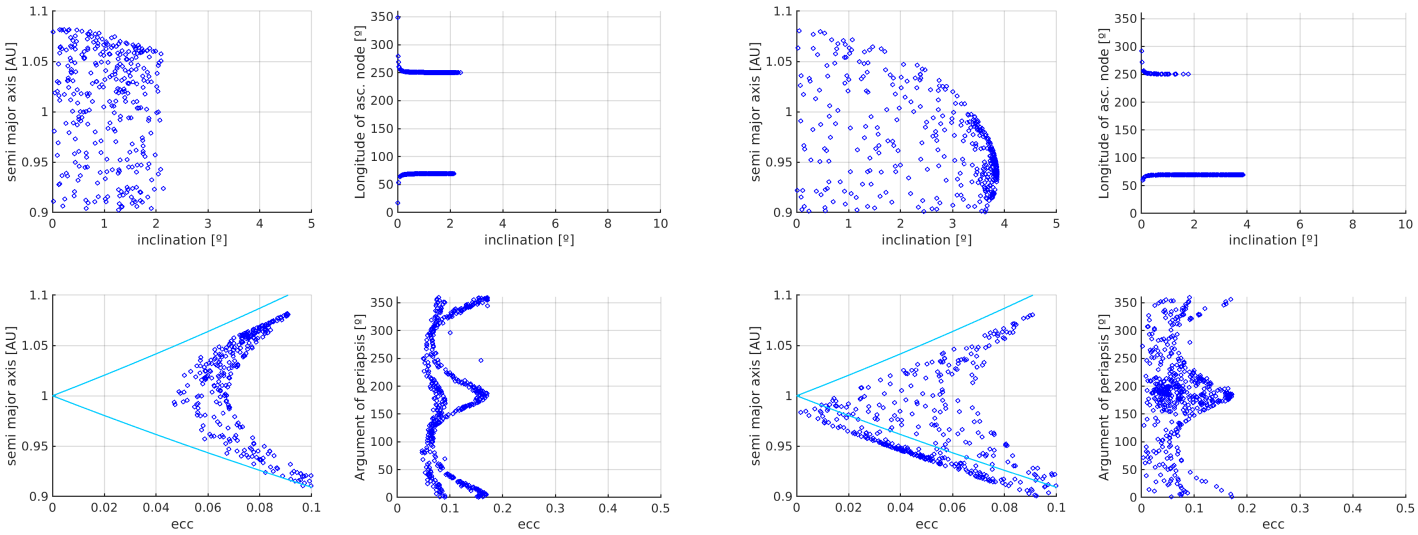

Figure A.14: Final orbital parameters, after 10^5 years. To the left the eastwards launch and to the right, northwards launch.

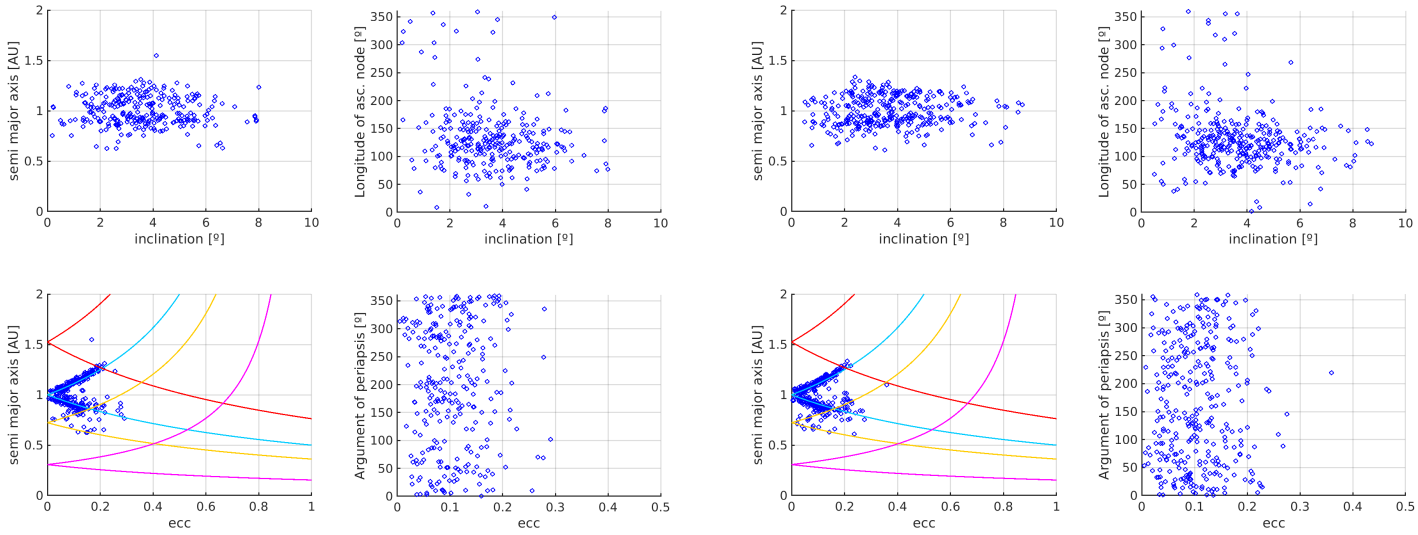

Figure A.15: Final orbital parameters, after 10^5 years. To the left the eastwards launch and to the right, northwards launch.

A.2.5 Case Study: Moon impact

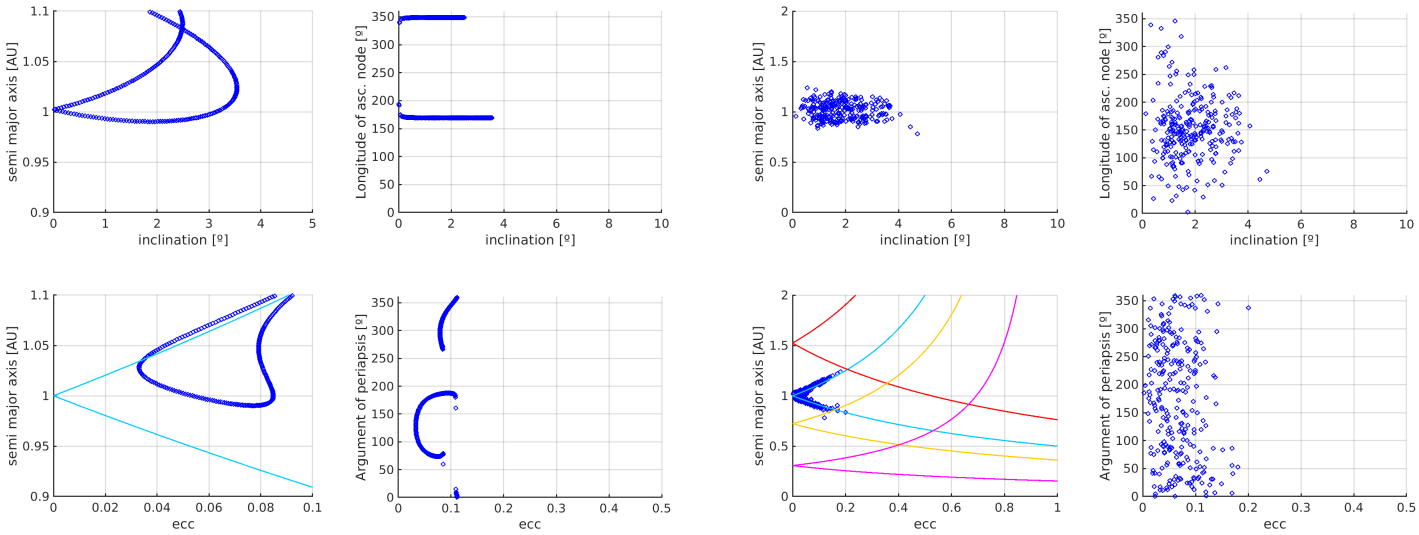

Figure A.16: Initial and final orbital parameters, after 10^4 years. To the left, orbital elements at first instant and to the right orbital elements at the end of the simulation.

A.3 Mineralogy

Sample Name	*Sample type*		Na2O	MgO	Al2O3	SiO2	CaO	TiO2	FeO
Apollo 11	Soils	Mare	0.47	7.90	12.60	42.00	11.70	7.90	16.40
Apollo 12	Soils	Mare	0.41	10.40	12.10	46.20	9.90	2.60	17.20
Apollo 15	Soils	Mare	0.40	11.00	14.30	47.20	10.50	1.46	15.00
Apollo 17	Soils	Mare	0.39	9.80	12.10	40.80	11.10	8.50	16.60
Luna 16	Core	Mare	0.38	8.80	15.60	44.40	11.70	3.30	16.40
Luna 24	Core	Mare	0.29	9.90	11.90	44.60	11.40	01.04	19.20
NWA 773	Regolith Breccia	Mare	0.23	13.20	10.60	46.20	10.80	0.78	17.30
QUE 94281	Regolith Breccia	Mainly mare	0.37	8.50	15.80	47.50	12.50	0.71	14.10
Yamato-793274	Regolith Breccia	Mainly mare	0.38	9.10	15.30	47.90	12.20	0.61	14.20
Apollo 14	Soil	Mainly highland	0.69	9.20	17.70	48.20	11.00	1.72	10.40
Apollo 15, Apennine Front	Core soil	Mainly highland	0.47	10.30	20.00	46.20	11.40	1.24	10.00
Apollo 17, South Massif	Soil	Mainly highland	0.42	9.70	21.30	45.20	13.00	1.22	8.00
Luna 20	Core soil	Mainly highland	0.38	9.20	23.00	45.00	14.40	0.46	7.30
Calcalong Creek	Regolith Breccia	Mainly highland	0.49		20.90		16.10	0.80	10.90
ALH 81005	Regolith Breccia	Highland	0.30	8.20	25.60	45.70	15.00	0.25	5.40
Apollo 14, 14076	Regolith Breccia	Highland	0.44	3.30	30.50	44.10	16.80	0.33	3.80
Apollo 14, 14315	Regolith Breccia	Highland	0.57	7.90	22.10	47.10	13.00	0.85	7.40
Apollo 16 average	Soils	Highland	0.48	5.80	27.10	44.70	15.50	0.58	5.20
Dar el Gani 262	Regolith Breccia	Highland	0.36	4.70	27.70	44.60	16.10	0.20	4.30
Dhofar 025	Regolith Breccia	Highland	0.31	6.50	26.80	44.50	15.80	0.29	4.80
MAC 88104/5	Regolith Breccia	Highland	0.33	4.00	28.10	45.00	16.60	0.24	4.20
QUE 93069	Regolith Breccia	Highland	0.34	4.60	28.50	44.90	16.30	0.27	4.30
Yamato 791197	Regolith Breccia	Highland	0.33	6.30	26.00	43.70	15.50	0.34	6.50
		Mare							
		average	0.37	9.84	13.37	45.20	11.31	2.99	16.27
		min	0.23	7.90	10.60	40.80	9.90	0.61	14.10
		max	0.47	13.20	15.80	47.90	12.50	8.50	19.20
		median	0.38	9.80	12.60	46.20	11.40	1.46	16.40
		Highland							
		average	0.42	6.90	24.66	45.30	14.75	0.63	6.61
		min	0.30	3.30	17.70	43.70	11.00	0.20	3.80
		max	0.69	10.30	30.50	48.20	16.80	1.72	10.90
		median	0.40	6.50	25.80	45.00	15.50	0.40	5.95

Table A.1: Chemical composition in wt % for lunar meteorites, lunar regoliths. Extracted from Table 2 of [4].

Sample Name	Na2O	MgO	Al2O3	SiO2	K2O	CaO	TiO2	FeO
Dhofar 287	0.52	12.30	8.10	43.90	0.11	8.40	2.86	22.20
Kalahari 9	0.53	8.50	12.80	46.20	0.19	10.50	0.45	15.90
LAP 2204	0.37	6.70	9.80	45.30	0.08	11.10	3.14	22.20
MIL 5035	0.24	7.60	9.10	47.70	0.02	12.00	1.17	21.40
NEA 3	0.29	13.60	8.00	44.70	0.08	9.20	1.34	20.60
NWA 32	0.35	7.90	9.10	44.70	0.11	10.90	3.10	22.00
NWA 773	0.14	26.70	4.40	43.00	0.09	5.60	0.32	19.40
NWA 4898	0.31	8.30	12.00	46.20	11.40	2.39	17.30	97.80
YA meteorite	0.32	6.00	11.00	45.50	0.05	12.00	2.10	22.30
Apollo 11	0.48	7.60	9.60	40.50	0.16	11.10	10.50	19.50
Apollo 12	0.27	10.80	9.30	45.10	0.06	10.00	3.40	20.40
Apollo 14	0.49	9.50	12.70	48.20	0.30	10.70	2.50	16.20
Apollo 15	0.27	10.40	9.10	46.30	0.05	9.80	2.10	21.20
Luna 16	0.52	6.40	13.40	43.80	0.18	11.70	5.00	18.70
Luna 24	0.27	9.40	11.20	45.70	0.03	11.60	0.80	20.10
Apollo 17 (high-Ti)	0.39	8.40	8.90	38.90	0.06	10.50	12.10	18.90
Apollo 17 VLT	0.15	12.50	10.40	48.20	0.02	9.40	0.70	18.30
All Apollo/Luna	0.35	9.40	10.60	44.60	0.11	10.60	4.70	19.10
average	0.35	10.11	9.97	44.92	0.73	9.86	04.09	24.23
min	0.14	6.00	4.40	38.90	0.02	2.39	0.32	15.90
max	0.53	26.70	13.40	48.20	11.40	12.00	17.30	97.80
median	0.34	8.95	9.70	45.20	0.09	10.55	2.68	20.25

Table A.2: Chemical composition in wt % for lunar meteorites, mare basalts. Extracted from Table 1 of [4].

The two previous tables retrieve the information provided by *Warren and Taylor* [4] on the compositional data of lunar meteorites. The database has been used as well as with Figure A.17 to consider the most probable origin region of the sample meteorites.

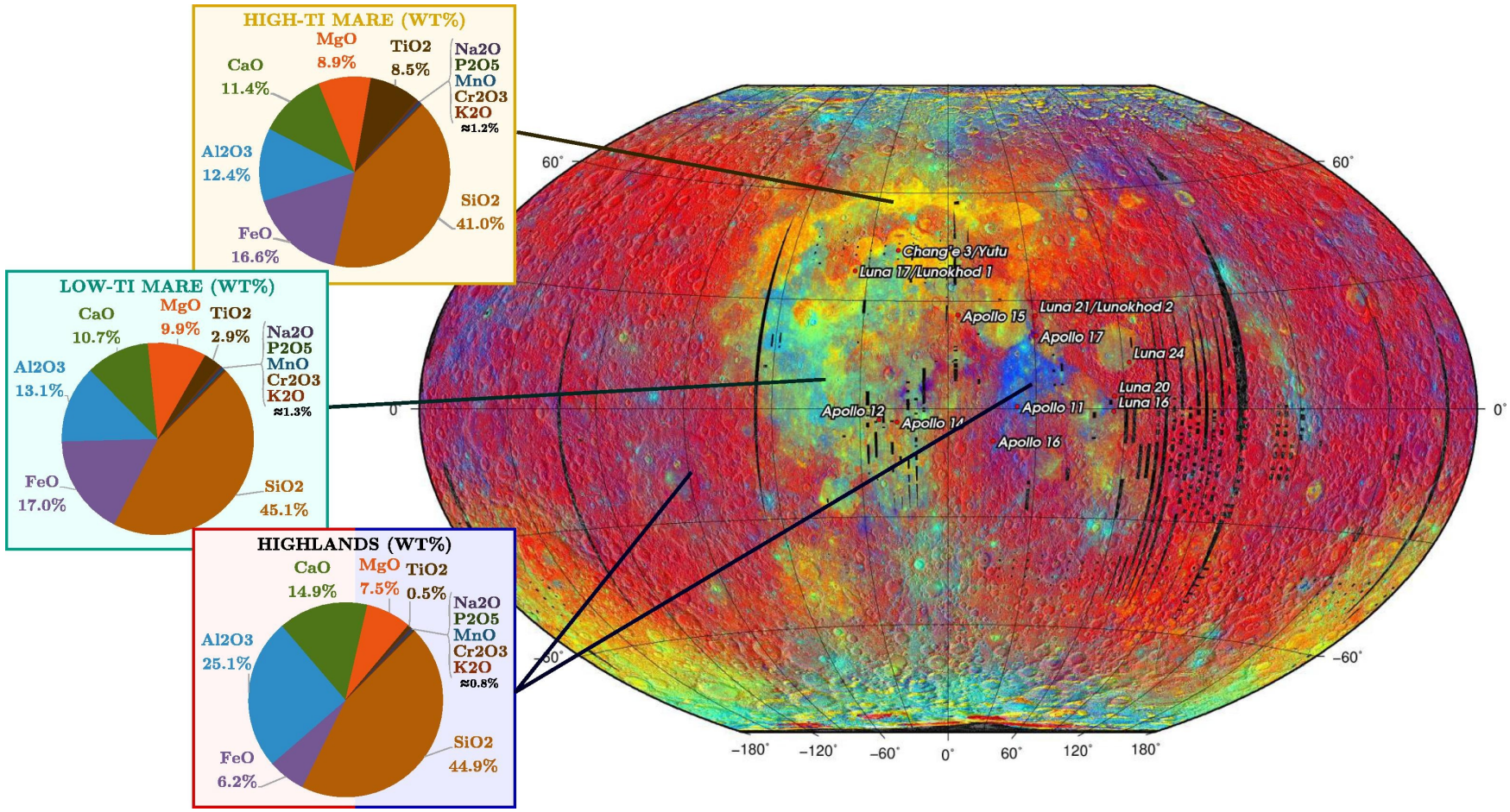

Figure A.17: Composition of the lunar surface. Two areas are distinguished, the highlands and the lunar maria, in turn, divided into high-Ti and low-Ti mare. Additionally, the map shows the location of the landing sites for US (Apollo), Russian (Luna) and Chinese (Chang'e) missions. Image extracted from [6].

A.3.1 Comparison of meteorites composition

	Na2O	MgO	Al2O3	SiO2	K2O	CaO	TiO2	FeO	
average	0.35	10.11	9.97	44.92	0.73	9.86	04.09	24.23	
min	0.14	6.00	4.40	38.90	0.02	2.39	0.32	15.90	
max	0.53	26.70	13.40	48.20	11.40	12.00	17.30	97.80	
median	0.34	8.95	9.70	45.20	0.09	10.55	2.68	20.25	
JaH 838 av.	0.35	4.75	16.66	46.64	0.00	9.78	0.23	11.75	**MSE**
	0.00	-5.36	6.69	1.72	-0.73	-0.08	-3.86	-12.48	30.96
	0.02	-4.20	6.96	1.44	-0.09	-0.77	-2.45	-8.50	18.38
DHO 1084 av.	0.59	7.71	6.00	46.62	1.86	3.13	8.57	8.14	**MSE**
	0.24	-2.40	-3.97	1.70	1.13	-6.73	4.48	-16.09	43.77
	0.26	-1.24	-3.70	1.42	1.78	-7.42	5.89	-12.11	32.11
NWA 11444 av.	0.11	9.57	15.72	42.06	0.00	10.33	0.14	11.90	**MSE**
	-0.24	-0.54	5.75	-2.86	-0.73	0.47	-3.95	-12.33	26.25
	-0.23	0.62	06.02	-3.14	-0.09	-0.22	-2.54	-8.35	15.35

Table A.3: Comparison between meteorite samples and mare basalts. Chemical components in wt %. MSE states for Mean Square Error. Data obtained from [4] Table 1.

	Na2O	MgO	Al2O3	SiO2	CaO	TiO2	FeO	
average	0.37	9.84	13.37	45.20	11.31	2.99	16.27	
min	0.23	7.90	10.60	40.80	9.90	0.61	14.10	
max	0.47	13.20	15.80	47.90	12.50	8.50	19.20	
median	0.38	9.80	12.60	46.20	11.40	1.46	16.40	
JaH 838 av.	0.35	4.75	16.66	46.64	9.78	0.23	11.75	**MSE**
	-0.02	-5.09	3.29	1.44	-1.53	-2.76	-4.52	9.89
	-0.03	-5.05	04.06	0.44	-1.62	-1.23	-4.65	9.71
DHO 1084 av.	0.59	7.71	6.00	46.62	3.13	8.57	8.14	**MSE**
	0.22	-2.13	-7.37	1.42	-8.18	5.58	-8.13	32.14
	0.21	-2.09	-6.60	0.42	-8.27	7.11	-8.26	33.62
NWA 11444 av.	0.11	9.57	15.72	42.06	10.33	0.14	11.90	**MSE**
	-0.26	-0.27	2.35	-3.14	-0.98	-2.85	-4.37	6.24
	-0.27	-0.23	3.12	-4.14	-1.07	-1.32	-4.50	7.16

Table A.4: Comparison between meteorite samples and mare regolith breccias. Chemical components in wt %. MSE states for Mean Square Error. Data obtained from [4] Table 2.

	Na2O	MgO	Al2O3	SiO2	CaO	TiO2	FeO	
average	0.42	6.90	24.66	45.30	14.75	0.63	6.61	
min	0.30	3.30	17.70	43.70	11.00	0.20	3.80	
max	0.69	10.30	30.50	48.20	16.80	1.72	10.90	
median	0.40	6.50	25.80	45.00	15.50	0.40	5.95	
JaH 838 av.	0.35	4.75	16.66	46.64	9.78	0.23	11.75	**MSE**
	-0.07	-2.15	-8.00	1.34	-4.97	-0.40	5.14	17.40
	-0.05	-1.75	-9.14	1.64	-5.72	-0.17	5.80	22.24
DHO 1084 av.	0.59	7.71	6.00	46.62	3.13	8.57	8.14	**MSE**
	0.17	0.81	-18.66	1.32	-11.62	7.94	1.53	78.75
	0.19	1.21	-19.80	1.62	-12.37	8.17	2.19	88.68
NWA 11444 av.	0.11	9.57	15.72	42.06	10.33	0.14	11.90	**MSE**
	-0.31	2.67	-8.94	-3.24	-4.42	-0.49	5.29	20.79
	-0.29	03.07	-10.08	-2.94	-5.17	-0.26	5.95	25.99

Table A.5: Comparison between meteorite samples and highland regolith. Chemical components in wt %. MSE states for Mean Square Error. Data obtained from [4] Table 2.

	Na2O	MgO	Al2O3	SiO2	K2O	CaO	TiO2	FeO	
average	0.60	8.90	12.40	44.10	0.60	11.40	8.50	16.60	
JaH 838 av.	0.35	4.75	16.66	46.64	0.00	9.78	0.23	11.75	**MSE**
	-0.25	-4.15	4.26	2.54	-0.60	-1.62	-8.27	-4.85	17.10
DHO 1084 av.	0.59	7.71	6.00	46.62	1.86	3.13	8.57	8.14	**MSE**
	-0.01	-1.19	-6.40	2.52	1.26	-8.27	0.07	-8.46	23.79
NWA 11444 av.	0.11	9.57	15.72	42.06	0.00	10.33	0.14	11.90	**MSE**
	-0.49	0.67	3.32	-2.04	-0.60	-1.07	-8.36	-4.70	13.67

Table A.6: Comparison between meteorite samples and high-Ti mare. Chemical components in wt %. MSE states for Mean Square Error. Data obtained from [6].

	Na2O	MgO	Al2O3	SiO2	K2O	CaO	TiO2	FeO	
average	0.65	9.90	13.10	45.10	0.65	10.70	2.90	17.00	
JaH 838 av.	0.35	4.75	16.66	46.64	0.00	9.78	0.23	11.75	**MSE**
	-0.30	-5.15	3.56	1.54	-0.65	-0.92	-2.67	-5.25	9.70
DHO 1084 av.	0.59	7.71	6.00	46.62	1.86	3.13	8.57	8.14	**MSE**
	-0.06	-2.19	-7.10	1.52	1.21	-7.57	5.67	-8.86	28.37
NWA 11444 av.	0.11	9.57	15.72	42.06	0.00	10.33	0.14	11.90	**MSE**
	-0.54	-0.33	2.62	-3.04	-0.65	-0.37	-2.76	-5.10	6.34

Table A.7: Comparison between meteorite samples and low-Ti mare. Chemical components in wt %. MSE states for Mean Square Error. Data obtained from [6].

	Na2O	MgO	Al2O3	SiO2	K2O	CaO	TiO2	FeO	
average	0.40	7.50	25.10	44.90	0.40	14.90	0.50	6.20	
JaH 838 av.	0.35	4.75	16.66	46.64	0.00	9.78	0.23	11.75	**MSE**
	-0.05	-2.75	-8.44	1.74	-0.40	-5.12	-0.27	5.55	17.38
DHO 1084 av.	0.59	7.71	6.00	46.62	1.86	3.13	8.57	8.14	**MSE**
	0.19	0.21	-19.10	1.72	1.46	-11.77	08.07	1.94	72.18
NWA 11444 av.	0.11	9.57	15.72	42.06	0.00	10.33	0.14	11.90	**MSE**
	-0.29	02.07	-9.38	-2.84	-0.40	-4.57	-0.36	5.70	19.26

Table A.8: Comparison between meteorite samples and highland samples. Chemical components in wt %. MSE states for Mean Square Error. Data obtained from [6].

	Na2O	MgO	Al2O3	SiO2	CaO	TiO2	FeO	
	0.40	1.21	33.40	45.57	19.10	0.08	1.00	
JaH 838 Spectra 5, 6	0.43	0.86	33.87	44.91	18.37	0.00	0.02	**MSE**
	-0.03	0.35	-0.47	0.66	0.73	0.08	0.98	0.33
NWA 11444 ROI 1 Spectra 1, 2	0.30	1.25	33.92	45.57	18.12	0.00	0.65	**MSE**
	0.10	-0.04	-0.52	0.00	0.98	0.08	0.35	0.20
NWA 11444 ROI 2 Spectra 3	0.37	1.44	32.89	44.97	19.52	0.00	0.14	**MSE**
	0.03	-0.23	0.51	0.60	-0.42	0.08	0.86	0.23
NWA 11444 ROI 3 Spectra 6, 7	0.34	6.25	26.26	47.35	15.53	0.00	4.22	**MSE**
	0.06	-5.04	7.14	-1.78	3.57	0.08	-3.22	14.67
NWA 11444 ROI 3 Spectra 9	0.44	1.51	34.48	44.64	17.87	0.00	0.94	**MSE**
	-0.04	-0.30	-1.08	0.93	1.23	0.08	0.06	0.52

Table A.9: Comparison between meteorite samples and an anorthosite sample. Chemical components in wt %. MSE states for Mean Square Error. Data obtained from [5].

A.3.2 SEM/EDX Analysis JaH 838

Spectrum 1 and Spectrum 2

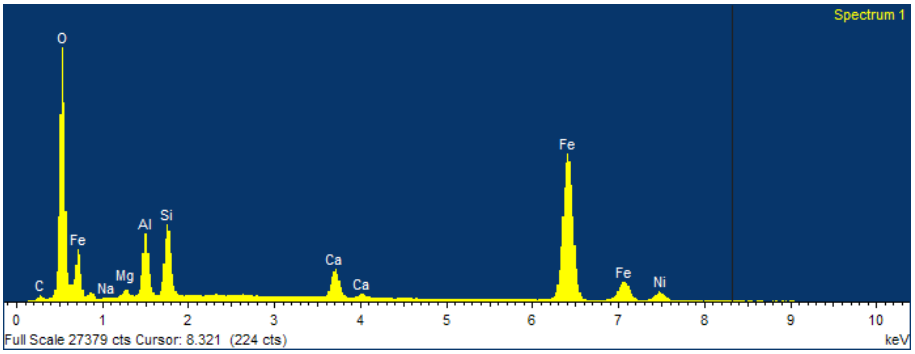

(a) Spectrum 1 JaH 838

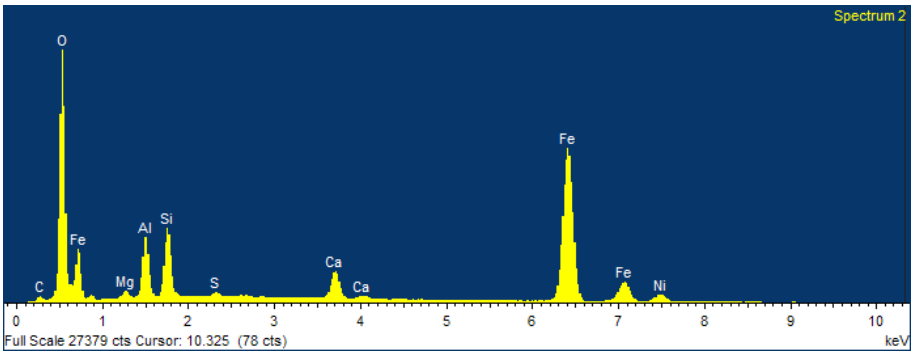

(b) Spectrum 2 JaH 838

Figure A.18: X-Ray Spectra 1 and 2 of JaH 838

	Spectrum 1		Spectrum 2		Average	
Element	**Weight %**	**Atomic %**	**Weight %**	**Atomic %**	**Weight %**	**Atomic %**
C	2.87	6.06	2.82	5.98	2.845	6.02
O	38.75	61.5	38.79	61.73	38.77	61.615
Na	0.22	0.24	0.68	0.71	0.45	0.475
Mg	0.74	0.78	4.92	4.64	2.83	2.71
Al	5.11	4.81	5.27	4.78	5.19	4.795
Si	5.48	4.95	0.33	0.26	2.905	2.605
Ca	2.68	1.7	2.62	1.67	2.65	1.685
Fe	38.85	17.67	40.62	18.52	39.735	18.095
Ni	5.3	2.29	3.95	1.71	4.625	2
Totals	100	100	100	100		

Table A.10: Spectrum 1 and 2 results for SEM/EDX microscopy

Both Spectrum 1 and Spectrum 2 are located in the same area, a whitish grain embedded in the matrix of JaH 838. Its brightness its due to the high percentage of Fe that it

contains. However, none of the spectra converge to a solution. Candidate minerals are: anorthite, fayalite and kamacite.

Spectrum 3

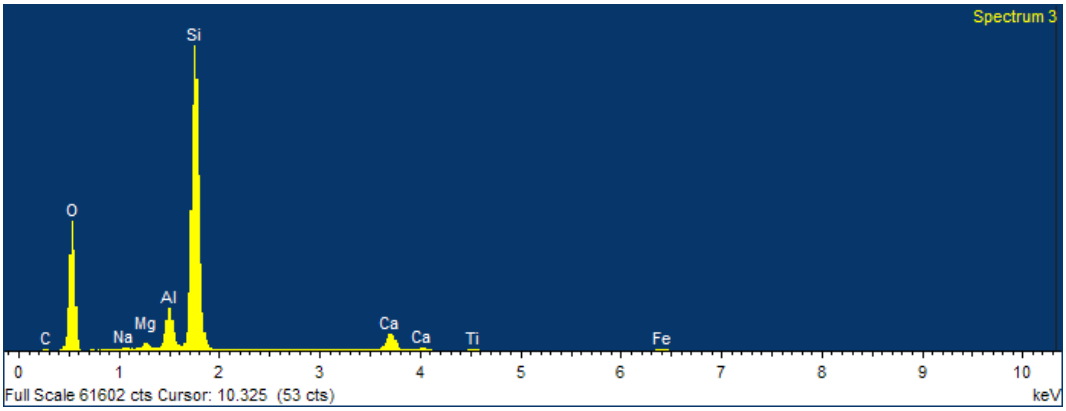

Figure A.19: X-Ray Spectrum 3 of JaH 838

Element	Weight %	Atomic %
C	2.36	3.86
O	54.21	66.61
Na	0.14	0.12
Mg	0.71	0.57
Al	4.18	3.05
Si	33.90	23.73
Ca	3.36	1.65
Ti	0.16	0.07
Fe	1.00	0.35
Totals	100.00	100.00

Table A.11: Spectrum 3 results for SEM/EDX microscopy

Spectrum 3 is located in JaH 838 matrix, but in particular a darker spot. Residuals are beyond the acceptable limit but MINSQ does not predict any extra chemical component that is not found in the sample. The main sources of error are the estimated proportions of Si, Mg, Ca and Na. Candidate minerals with their expected proportions are:

- Albite 85.9 %
- Clinoenstatite 10.3 %
- Pigeonite 3.8 %

It can be concluded that the sample area has as predominant mineral albite with secondary minerals (probably clinoenstatite and pigeonite).

Spectrum 4

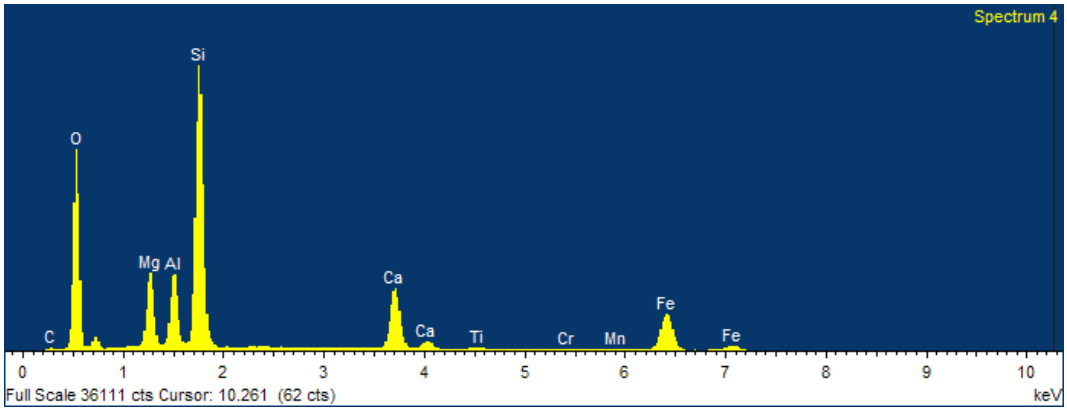

Figure A.20: X-Ray Spectrum 4 of JaH 838

Spectrum 4 also is located on the matrix but in a brighter region. This indicates a more abundant presence of Fe than in comparison than Spectrum 5 and 6. Candidate minerals with their respective estimations are:

- Albite 4 %
- Augite 32.6 %
- Pigeonite 29.4 %
- Ferrosilite 2.4 %
- Labradorite 28.8 %
- Kamacite 6.8 %
- Others $<$ 1% (not included)

Element	**Weight %**	**Atomic %**
C	2.26	3.98
O	48.13	63.65
Mg	5.84	5.08
Al	5.11	4.00
Si	20.39	15.36
Ca	6.60	3.48
Ti	0.32	0.14
Cr	0.19	0.08
Mn	0.17	0.07
Fe	10.98	4.16
Totals	100.00	100.00

Table A.12: Spectrum 4 results for SEM/EDX microscopy

Firstly, kamacite is discarded as there is no Ni found in the sample. On the other hand, the absence of Na supports the presence of feldspars anorthite and labradorite. The presence of augite could be the cause of a peak in Si as well as a pigeonite rich in Mg and with ions of Fe. Particularly, the peak of Fe at 6.5 keV characterises Mg-Fe pyroxenes.

Spectrum 5 and Spectrum 6

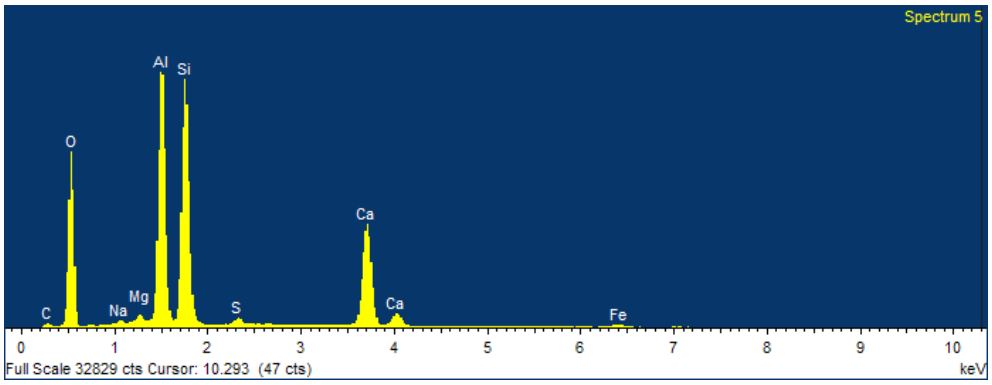

(a) Spectrum 5 JaH 838

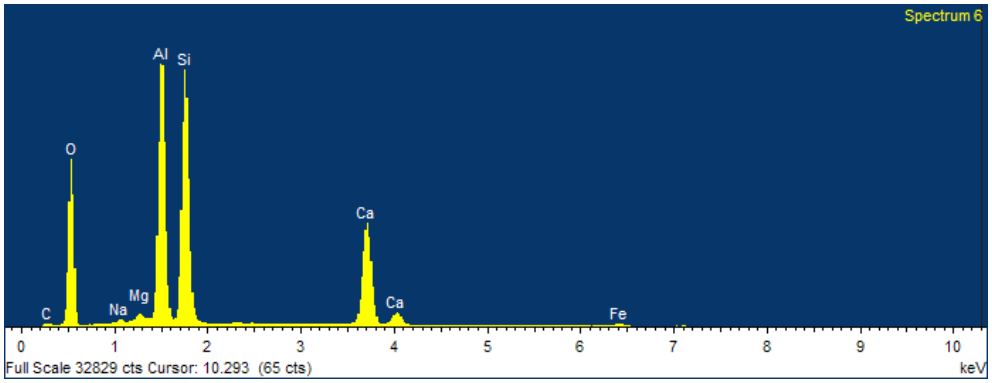

(b) Spectrum 6 JaH 838

Figure A.21: X-Ray Spectra 5 and 6 of JaH 838

	Spectrum 5		Spectrum 6		Average	
Element	**Weight %**	**Atomic %**	**Weight %**	**Atomic %**	**Weight %**	**Atomic %**
C	3.44	5.75	2.54	4.3	2.99	5.025
O	50.7	63.65	50.07	63.59	50.385	63.62
Na	0.28	0.25	0.27	0.24	0.275	0.245
Mg	0.42	0.35	0.48	0.4	0.45	0.375
Al	15.06	11.21	15.82	11.91	15.44	11.56
Si	17.62	12.6	18.7	13.52	18.16	13.06
S	0.53	0.33				
Ca	11.12	5.57	11.37	5.76	11.245	5.665
Fe	0.84	0.3	0.74	0.27	0.79	0.285
Totals	100	100	100	100		

Table A.13: Spectrum 5 results for SEM/EDX microscopy

Spectrum 5 and Spectrum 6 are pointing to the meteorite's matrix but being ≈200 μm from each other. Their composition is almost identical except for the presence of S in Spectrum 5 (in less than 1% in weight). Spectrum 6 hints also the presence of S with an

extremely small peak at the same location, but going undetected.

The mineral candidates for the averaged spectrum are:

- Anorthite 90.2 %
- Augite 2 %
- Clinoenstatite 1.7%
- Pyrrhotite 1.1%
- Labradorite 5.1 %

This case is clearly a plagioclase anorthite due to the *twin* peaks of Al and Si and the lesser peak of Ca (at approximately half of the peak of Al and Si). The rest of minerals calculated try to include the rest of the elements that appear such as Fe, Mg and Na but the sample should be further analysed to reliably determine them. In particular the mineral containing S, which is suggested to be pyrrhotite, but needs further analysis for identification.

Mapping

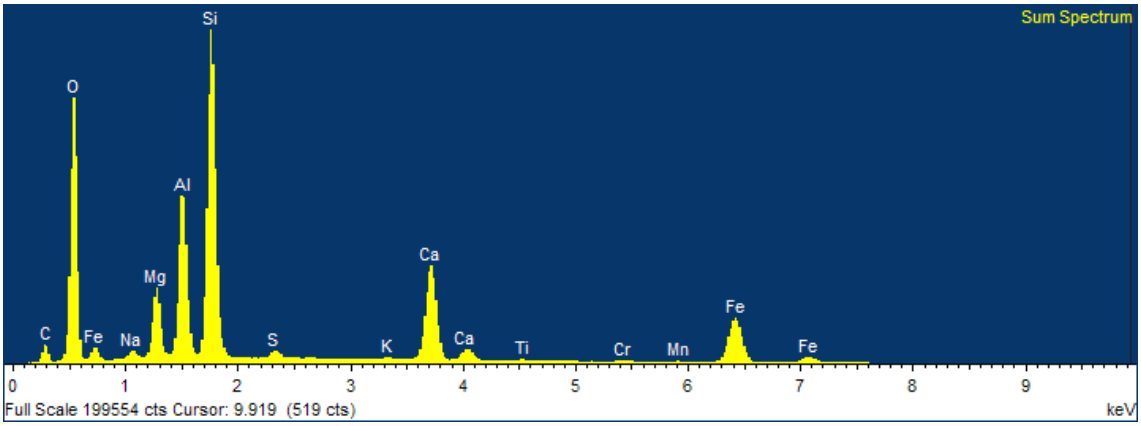

Figure A.22: X-Ray Spectrum of the mapping of JaH 838

The spectrum of the mapping is the sum of all spectra for the region analysed, hence, will not describe the elements in a particular point like the previous spectra but an averaged value of the whole region. Thus, interpretation directly from the X-Rays pattern becomes more difficult, being more suitable the direct interpretation of the mappings.

In the electron image 3.3.b two different patterns can be observed: a set of stripes-pattern in the left region and a set of small round clusters on the right upper side. The

easier way to start is finding *dark spots* (empty) in the brightest of maps, the Si mapping. According to Figure 3.5.f a dark cluster on the top right indicating an absence of Si stands out in the mappings of S and Fe. Thus, hinting the presence of FeS (troilite). On the lower right part of the Si mapping there is a particularly dark stripe that remains dark for all maps but for the Ca mapping. It indicates embedded calcium.

If observing the Mg mapping, there are regions (specially on the upper part) that coincide in brightness with the Fe mapping, furthermore, overlaying with Ca-poor spots and Si-rich spots. This region probably corresponds to a low-Ca pigeonite. The middle part of the image corresponds to the matrix of plagioclase anorthite (see that Al, Si and Ca remain homogeneous).

The dominant minerals with their estimations are the following:

- Anorthite 30.6 %
- Augite 17.4 %
- Pigeonite 20.6 %
- Ferrosilite 5.8 %
- Labradorite 19.6 %
- Troilite 1.8 %
- Kamacite 4.8 %
- Others $< 1\%$

Element	**Weight %**	**Atomic %**
C	8.36	13.89
O	47.00	58.61
Na	0.59	0.51
Mg	3.64	2.98
Al	7.42	5.49
Si	15.89	11.29
S	0.44	0.27
K	0.13	0.07
Ca	6.95	3.46
Ti	0.15	0.06
Cr	0.20	0.08
Mn	0.12	0.05
Fe	9.12	3.26
Totals	100.00	100.00

Table A.14: Spectrum-mapping results for SEM/EDX microscopy of JaH838

As stated before, despite the low mineral percentage, troilite was expected due to the concentrations of S and Fe in the same specific, small-defined regions. Kamacite, even though MINSQ predicts a greater percentage than troilite, is discarded as there is no presence of Ni detected. The plagioclase anorthite is the mineral with highest percentage (in weight). Taking into account that pigeonite and anorthite have similar molecular weights the result is in accordance with the previous hypotheses: the central part corresponds to a anorthite matrix and the top right clusters to the pigeonite.

A.3.3 SEM/EDX analysis of meteorite DHO 1084

Spectrum 1 and Spectrum 2

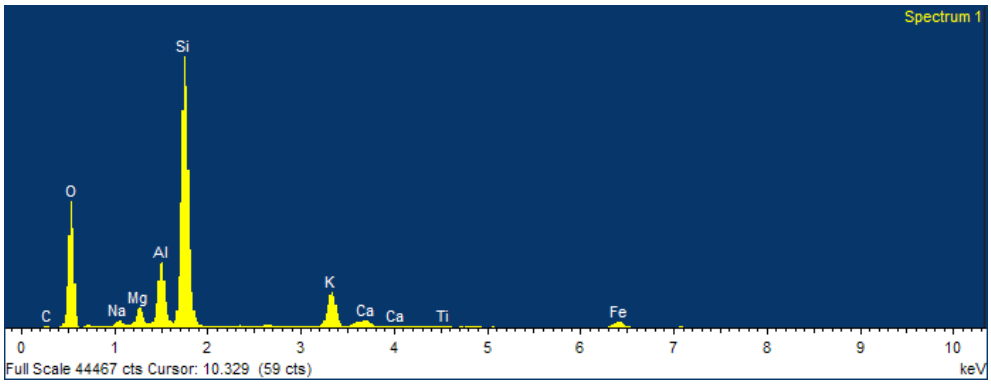

(a) Spectrum 1 of the mapping of DHO 1084

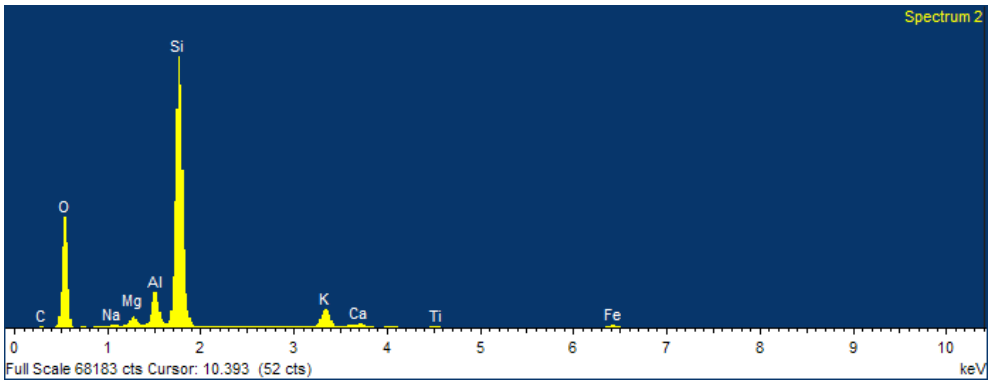

(b) Spectrum 2 of the mapping of DHO 1084

Figure A.23: X-Ray Spectra 1 and 2 of DHO 1084

	Spectrum 1		Spectrum 2		Average	
Element	**Weight %**	**Atomic %**	**Weight %**	**Atomic %**	**Weight %**	**Atomic %**
C	-0.17	-0.29	0.15	0.24	-0.01	-0.025
O	51.51	66.48	53.08	67.25	52.295	66.865
Na	0.87	0.79	0.4	0.35	0.635	0.57
Mg	2.02	1.72	1.24	1.03	1.63	1.375
Al	6.34	4.85	4.01	3.01	5.175	3.93
Si	29.51	21.69	34.7	25.05	32.105	23.37
K	5.88	3.11	3.95	2.05	4.915	2.58
Ca	1.04	0.53	0.72	0.36	0.88	0.445
Ti	0.2	0.09	0.12	0.05	0.16	0.07
Fe	2.79	1.03	1.63	0.59	2.21	0.81
Totals	100	100	100	100		

Table A.15: Spectra 1 and 2 results for SEM/EDX microscopy of DHO 1084

Spectra 1 and 2 are diametrically opposed one from the other but both point the meteorite's matrix, obtaining almost identical X-Ray spectra. Even though MINSQ results diverge, the main difference between theoretical and obtained values stems from the amounts in Na and K. The most probable explanation is that the ratios of Na and K found in the minerals do not fit with the ratios in the preallocated minerals. On one extreme there is the orthoclase, a potassium feldspar (K-feldspar) and on the other albite, with sodium; these ions can coexist in intermediate ratios. The candidate minerals and their estimations:

- Albite 80.4 %
- Pigeonite 9.9 %
- Kamacite 1.4 %

As previously mentioned, the matrix of this meteorite will be considered mainly as an orthoclase (70-80%) with an unspecified percentage of plagioclase albite giving as a result an alkali feldspar.

Spectrum 3 and Spectrum 4

	Spectrum 3		**Spectrum 4**		**Average**	
Element	**Weight %**	**Atomic %**	**Weight %**	**Atomic %**	**Weight %**	**Atomic %**
C	5.85	11.91	6.75	13.57	6.3	12.74
O	41.11	62.79	40.75	61.53	40.93	62.16
Na	0.5	0.53	0.29	0.31	0.395	0.42
Mg	0.55	0.55	0.85	0.84	0.7	0.695
Al	1.36	1.24	1.53	1.37	1.445	1.305
Si	14.33	12.46	13.66	11.75	13.995	12.105
K	0.98	0.61	0.73	0.45	0.855	0.53
Ca	0.81	0.49	1.33	0.8	1.07	0.645
Fe	1	0.44	2	0.87	1.5	0.655
Zr	33.51	8.98	32.1	8.5	32.805	8.74
Totals	100	100	100	100		

Table A.16: Spectra 3 and 4 results for SEM/EDX microscopy of DHO 1084

Spectra 3 and 4 are located in a two different white granules with sharp angles (resembling rectangles or rhomboids, in contrast to rounded, spherical granules). The main characteristic of these spectra is the presence of zirconium (Zr). The candidate minerals for the averaged spectrum are:

- Albite 5.2 %
- Augite 4 %
- Pigeonite 3.7 %

- Ferrosilite 0.7 %
- Labradorite 6.7 %
- Zircon 78.6 %
- Others <1 %

Both spectra are clear, the granules are incrustations of zircon ($ZiSiO_4$) with the rest of elements being secondary for the composition of the granules. One source of error still is owing to an unadjusted prediction of K. As in the previous case, this is to different ratios of Na and K found in the mineral. Hence, the percentage of plagioclase albite is split between a certain amount of albite and of orthoclase that defines an alkali feldspar.

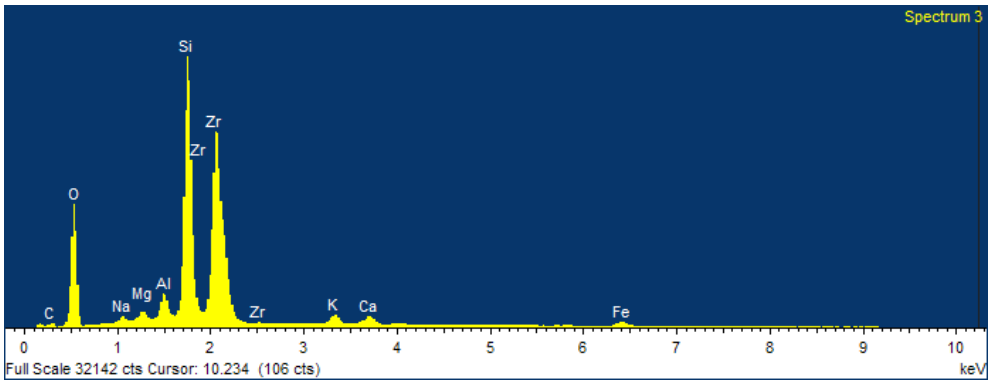

(a) Spectrum 3 of the mapping of DHO 1084

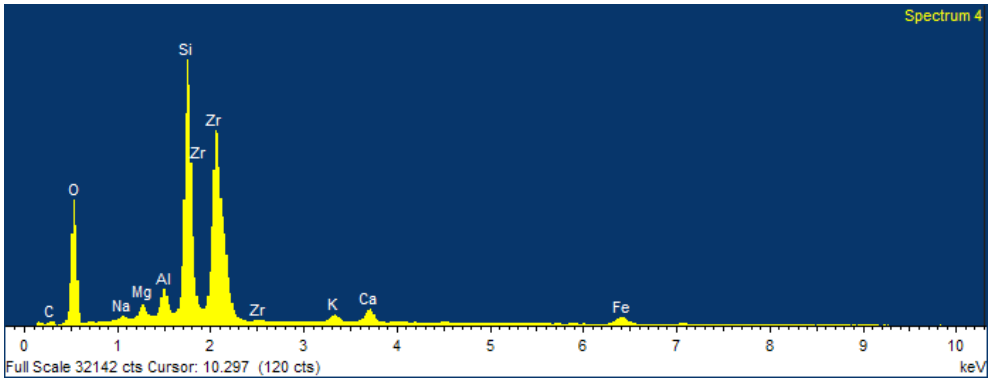

(b) Spectrum 4 of the mapping of DHO 1084

Figure A.24: X-Ray Spectrum 3 of DHO 1084

Spectrum 5 and Spectrum 6

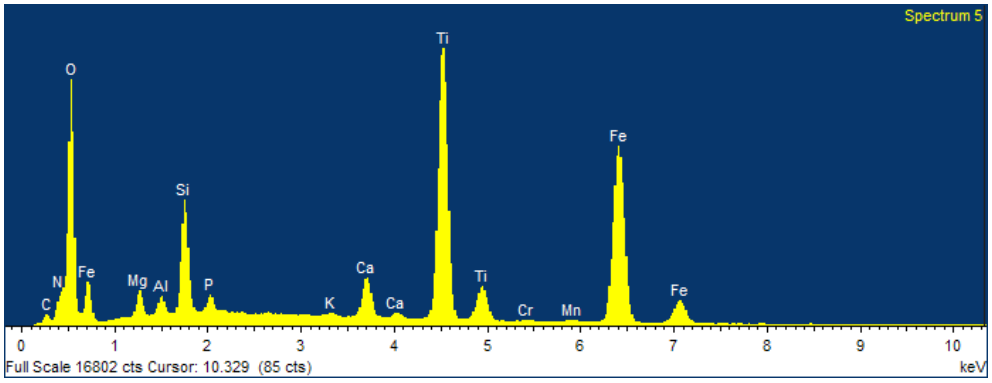

(a) Spectrum 5 of the mapping of DHO 1084

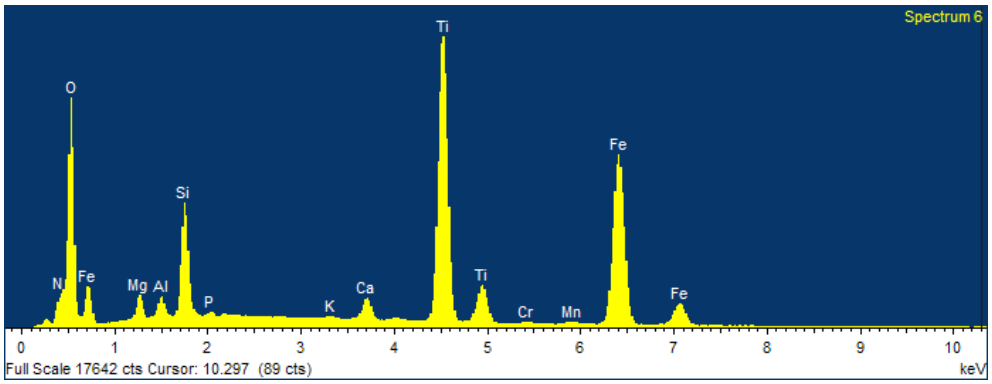

(b) Spectrum 6 of the mapping of DHO 1084

Figure A.25: X-Ray Spectra 5 and 6 of DHO 1084

	Spectrum 5		Spectrum 6		Average	
Element	**Weight %**	**Atomic %**	**Weight %**	**Atomic %**	**Weight %**	**Atomic %**
C	0.88	1.94				
N	-5.14	-9.75	-4.53	-8.71	-4.835	-9.23
O	44.13	73.3	43.62	73.46	43.875	73.38
Mg	1.44	1.58	1.43	1.59	1.435	1.585
Al	0.8	0.78	0.9	0.9	0.85	0.84
Si	4.56	4.32	4.74	4.55	4.65	4.435
P	0.83	0.71	0.21	0.19	0.52	0.45
K	0.14	0.1	0.14	0.09	0.14	0.095
Ca	2.12	1.4	1.17	0.79	1.645	1.095
Ti	21.72	12.05	23.75	13.36	22.735	12.705
Cr	0.19	0.1	0.2	0.11	0.195	0.105
Mn	0.26	0.12	0.26	0.13	0.26	0.125
Fe	28.07	13.36	28.1	13.55	28.085	13.455
Totals	100	100	100	100	100	

Table A.17: Spectra 5 and 6 results for SEM/EDX microscopy of DHO 1084

Spectra 5 and 6 are located in a bright region at the lower left of the image. This regions turns out to be rich in titanium (Ti) and iron (Fe).

The calculation with MINSQ is inconclusive, meaning that it does not converge and that specially low-percentage minerals are potentially wrong, either because they are missing or because have been added erroneously. The primary mineral is highly probable to be ilmenite, and above the 50% in wt.

Despite real percentages of the minerals might be different, this result the major peaks found in Ti and Fe and those in Si. The region is characterised by an iron-titanium oxide, predicted to be ilmenite, even though the Ti peak is particularly high.

Spectrum 7 and Spectrum 8

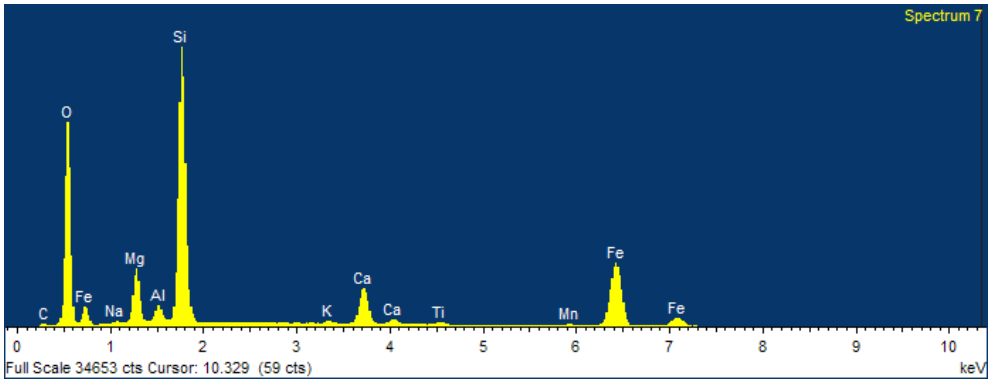

(a) Spectrum 7 of the mapping of DHO 1084

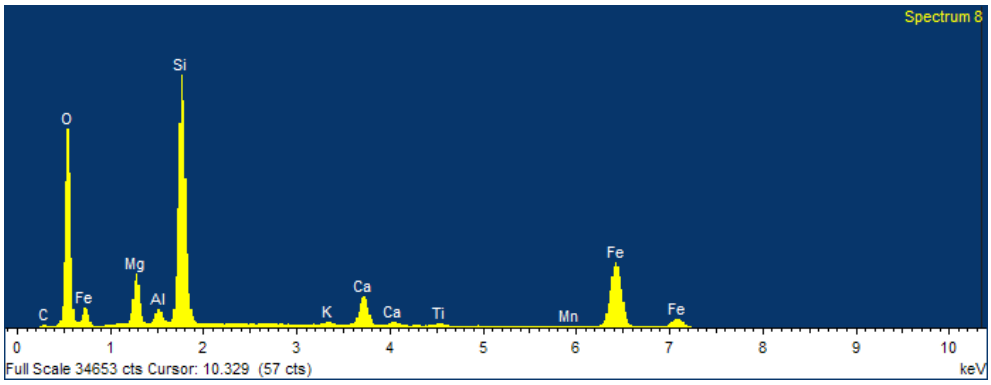

(b) Spectrum 8 of the mapping of DHO 1084

Figure A.26: X-Ray Spectra 7 and 8 of DHO 1084

Spectra 7 and 8 belong to a greyish region occupying half of the area of study. This area resembles a sort of crust and has many cracks in different directions, of a darker colour, that are intrusions of the matrix. For this spectrum the proportions of both Na and K differ from those of the sample pointing out to the same problem previously encountered:

	Spectrum 7		Spectrum 8		Average	
Element	**Weight %**	**Atomic %**	**Weight %**	**Atomic %**	**Weight %**	**Atomic %**
C	0.84	1.58	-0.38	-0.73	0.23	0.425
O	45.73	64.32	45.95	65.84	45.84	65.08
Na	0.26	0.25			0.26	0.25
Mg	5.12	4.74	5.24	4.94	5.18	4.84
Al	1.26	1.05	1.22	1.04	1.24	1.045
Si	21.25	17.03	21.1	17.22	21.175	17.125
K	0.28	0.16	0.26	0.15	0.27	0.155
Ca	4.21	2.36	3.68	2.11	3.945	2.235
Ti	0.41	0.19	0.35	0.17	0.38	0.18
Mn	0.33	0.14	0.28	0.12	0.305	0.13
Fe	20.29	8.17	22.3	9.15	21.295	8.66
Totals	100	100	100	100		

Table A.18: Spectra 7 and 8 results for SEM/EDX microscopy of DHO 1084

the real mineral is an alkali feldspar (in between K-feldspar and albite). Additionally, the solver erroneously predicts the presence of Zr, Ni and S forcing zircon, kamacite and troilite, respectively, to appear in the mineral estimates. The minerals calculated from elements that are not present in the SEM/EDX analysis are deprecated.

The mineral candidates for the averaged spectrum are:

- Albite 19.2%
- Augite 23.9 %
- Pigeonite 33.8 %
- Ferrosilite 16.8 %

The presence of augite with an intermediate amount of Mg complies with the X-Ray pattern, with peaks on both Ca and Fe. This case requires additional analysis (with Raman Spectroscopy) as the primary minerals have very similar weight percentages.

Spectrum 9

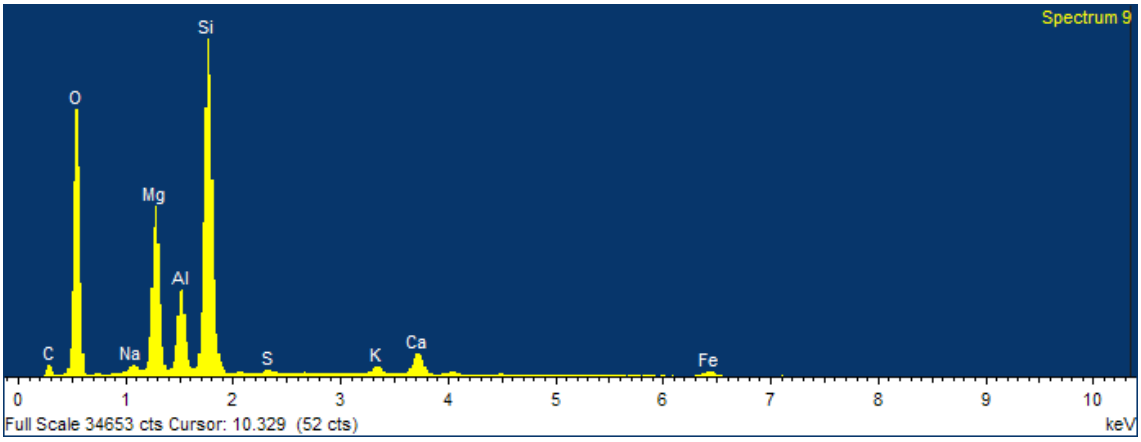

Figure A.27: X-Ray Spectrum 9 of DHO 1084

Spectrum 9 is located in a darker region where it seems the matrix has been scratched. This region is characterised by long semi-horizontal lines all of them in the same direction. In this spectrum it is also found a disadjustment in the proportions of Na and K and an unwanted presence in the solution of Ni and Zr which lead to mineral estimation of kamacite and zircon, respectively. Candidate minerals are:

- Albite 4.7%
- Clinoenstatite 55.1 %
- Labradorite 37.3 %
- Ferrosilite 2.7 %
- Others <1 %

Element	Weight %	Atomic %
C	10.29	15.71
O	51.50	59.06
Na	0.55	0.44
Mg	9.59	7.23
Al	4.64	3.16
Si	19.34	12.63
S	0.26	0.15
K	0.67	0.32
Ca	2.00	0.92
Fe	1.16	0.38
Totals	100.00	100.00

Table A.19: Spectrum 9 results for SEM/EDX microscopy of DHO 1084

A.3.4 Analysis SEM/EDX of meteorite NWA 11444

ROI 1: Spectrum 1 and 2

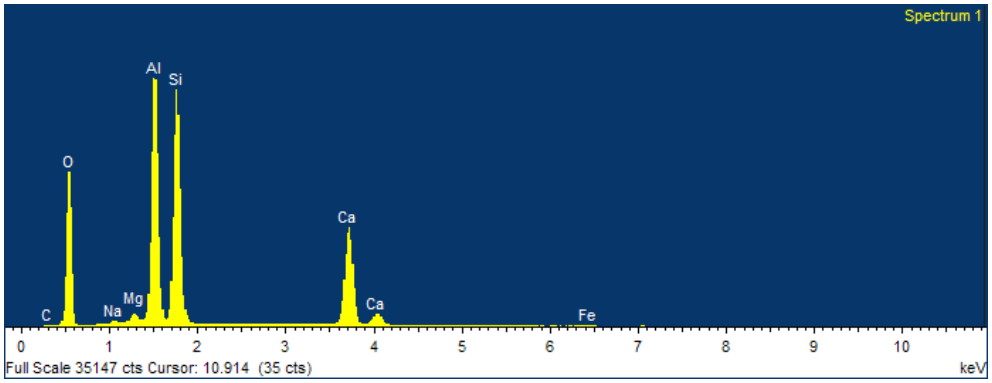

(a) Spectrum 1 of the mapping of NWA 11444 (ROI 1)

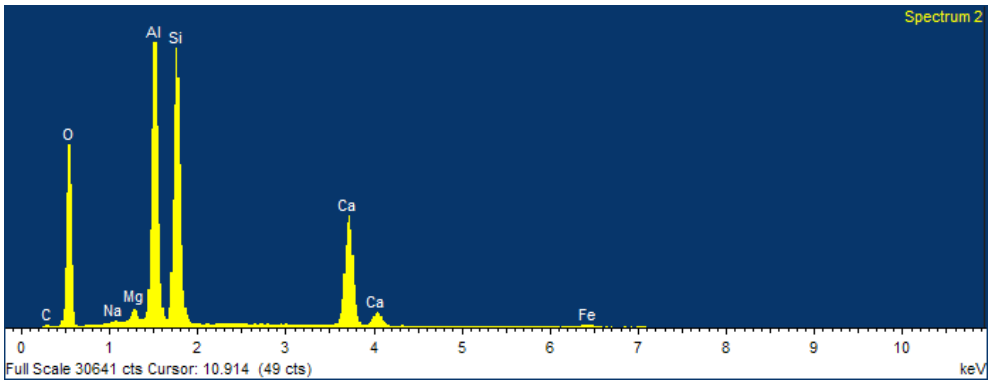

(b) Spectrum 2 of the mapping of NWA 11444 (ROI 2)

Figure A.28: X-Ray Spectra 1 and 2 of NWA 11444

	Spectrum 1		Spectrum 2		Average	
Element	**Weight %**	**Atomic %**	**Weight %**	**Atomic %**	**Weight %**	**Atomic %**
C	1.28	2.2	1.64	2.79	1.46	2.495
O	50.17	64.48	50.2	64.26	50.185	64.37
Na	0.2	0.18	0.2	0.18	0.2	0.18
Mg	0.59	0.5	0.77	0.65	0.68	0.575
Al	16.31	12.42	16.02	12.16	16.165	12.29
Si	18.99	13.9	18.97	13.83	18.98	13.865
Ca	11.95	6.13	11.5	5.87	11.725	6
Fe	0.5	0.19	0.71	0.26	0.605	0.225
Totals	100	100	100	100		

Table A.20: Spectra 1 and 2 results for SEM/EDX microscopy of NWA 11444 (ROI 1)

Spectra 1 and 2 (ROI 1) point to the matrix of the meteorite. The *twin peaks* of Al and Si along with a peak of Ca half of their size clearly indicates the presence of a plagioclase

anorthite. The mineral candidates for the averaged spectrum are:

- Anorthite 91.4 %
- Pigeonite 3.5 %
- Clinoenstatite 1.1 %
- Labradorite 4 %
- Others $<$ 1%, $<$1 %

The matrix can be concluded to be anorthite. The rest of the minerals, as they have low weight % should be also obtained by other methods (Raman Spectroscopy). The presence of labradorite could explain a small amount of Na and the peak of Al, being slightly larger than the peak of Si. The presence of Mg and Fe alongside with some ions of Ca's peak justify the presence of augite.

ROI 1: Spectrum 3 and Spectrum 4

	Spectrum 3		**Spectrum 4**		**Average**	
Element	**Weight %**	**Atomic %**	**Weight %**	**Atomic %**	**Weight %**	**Atomic %**
C	1.56	2.76	2.16	3.81	1.86	3.285
O	46.68	62.23	46.18	61.32	46.43	61.775
Mg	14.32	12.56	14.47	12.64	14.395	12.6
Al	3.81	3.01	3.47	2.73	3.64	2.87
Si	16.5	12.53	16.51	12.49	16.505	12.51
Ca	2.34	1.24	3.06	1.62	2.7	1.43
Mn	0.18	0.07				
Fe	14.63	5.59	14.15	5.38	14.39	5.485
Totals	100	100	100	100		

Table A.21: Spectra 3 and 4 results for SEM/EDX microscopy of NWA 11444 (ROI 1)

Spectra 3 and 4 are both inside a brighter region of the matrix, contained in a large granule. Their composition is almost identical except for the absence of Mn in Spectrum 4 (which probably is below the threshold of the microscope to be detected).

Looking at the X-Rays peaks of the spectrum, their distribution suggests a pyroxene group rich in Mg. The minerals along with their estimations are:

- Anorthite 21.8 %
- Pigoenite 7.5 %
- Clinoenstatite 7.9 %

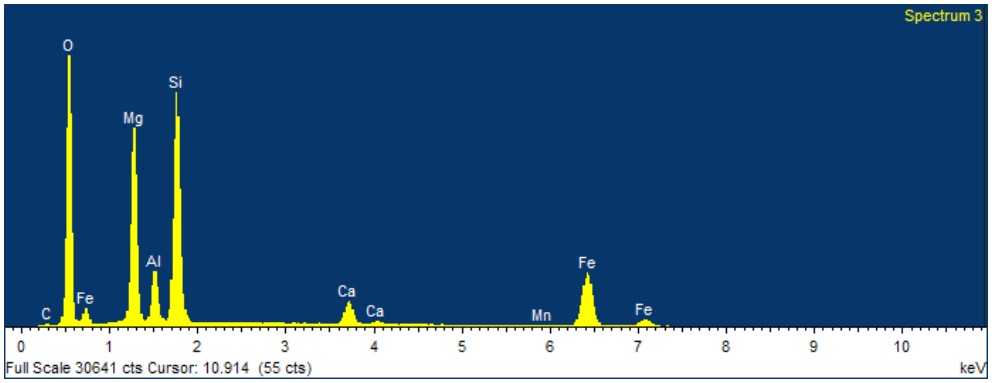

(a) Spectrum 3 of the mapping of NWA 11444 (ROI 1)

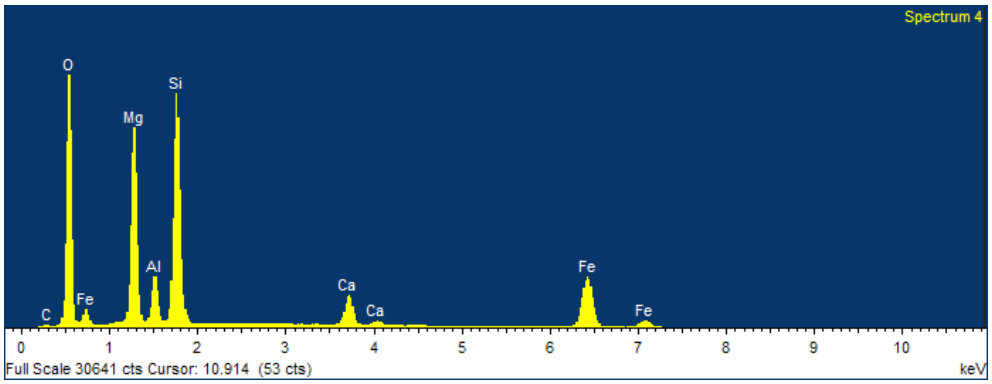

(b) Spectrum 4 of the mapping of NWA 11444 (ROI 1)

Figure A.29: X-Ray Spectra 3 and 4 of NWA 11444 (ROI 1)

- Ferrosilite 1.3 %
- Fayalite 15.4 %
- Olivine 39.4 %
- Kamacite 7% (deprecated)

The olivine fosterite supports the presence of Mg and Fe with a peak of Si. If the sample could be observed with a polarised microscope would allow to see the colours that make characteristic the olivine. As in other samples, some minerals have been deprecated as MINSQ predicted them from an element not found in the spectrum analysis. Those include: ilmenite, chromite, kamacite and troilite.

ROI 1: Spectrum 5 and Spectrum 6

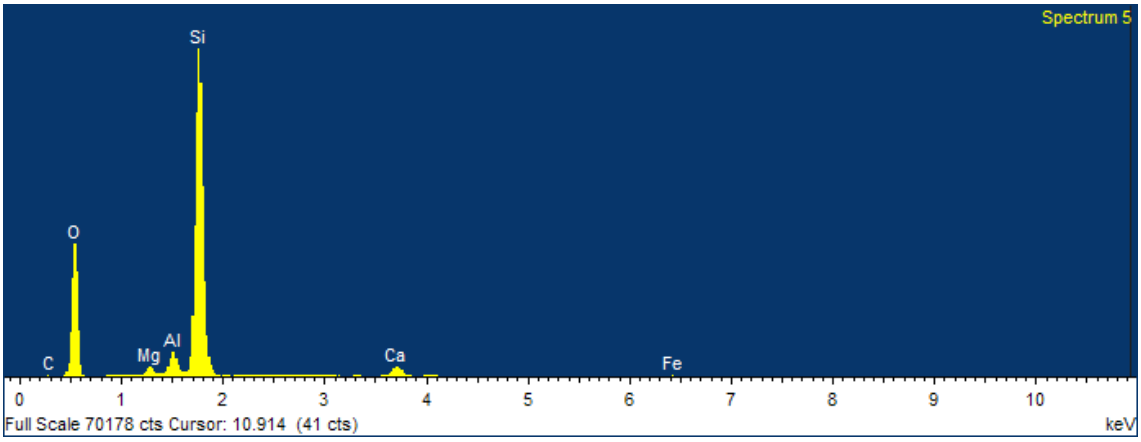

(a) Spectrum 5 of the mapping of NWA 11444 (ROI 1)

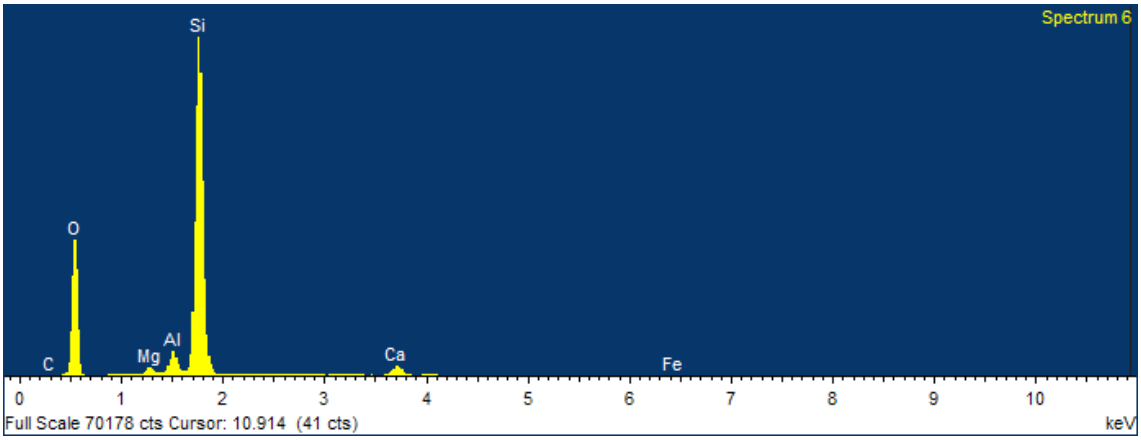

(b) Spectrum 6 of the mapping of NWA 11444 (ROI 1)

Figure A.30: X-Ray Spectra 5 and 6 of NWA 11444

	Spectrum 5		Spectrum 6		Average	
Element	**Weight %**	**Atomic %**	**Weight %**	**Atomic %**	**Weight %**	**Atomic %**
C	2.06	3.35	2.07	3.36	2.065	3.355
O	55.15	67.34	55.2	67.35	55.175	67.345
Mg	0.92	0.74	0.79	0.63	0.855	0.685
Al	2.32	1.68	2.18	1.58	2.25	1.63
Si	36.92	25.68	37.38	25.98	37.15	25.83
Ca	2.06	1	1.91	0.93	1.985	0.965
Fe	0.56	0.2	0.47	0.16	0.515	0.18
Totals	100	100	100	100		

Table A.22: Spectra 5 and 6 results for SEM/EDX microscopy of NWA 11444 (ROI 1)

Spectra 5 and 6 both are located in a darker region of the matrix, enclosed in a large grain and with particularly a fractured surface.

Particularly these samples do not converge on MINSQ, residual generated are well above the tolerance. If accepting MINSQ results, the region will be between 80% and 90% plagioclase albite, but then, there would be a set of ions of Na which are absent in the real analysis. This case needs additional analysis with Raman Spectroscopy.

ROI 1: Spectrum 7 and Spectrum 8

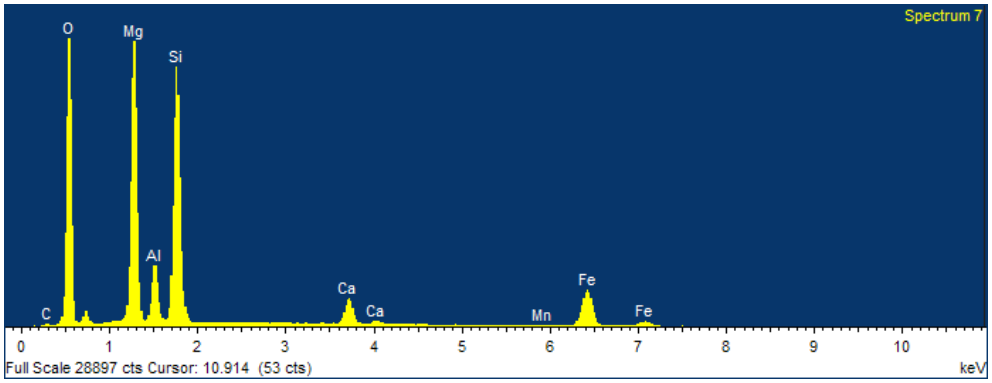

(a) Spectrum 7 of the mapping of NWA 11444 (ROI 1)

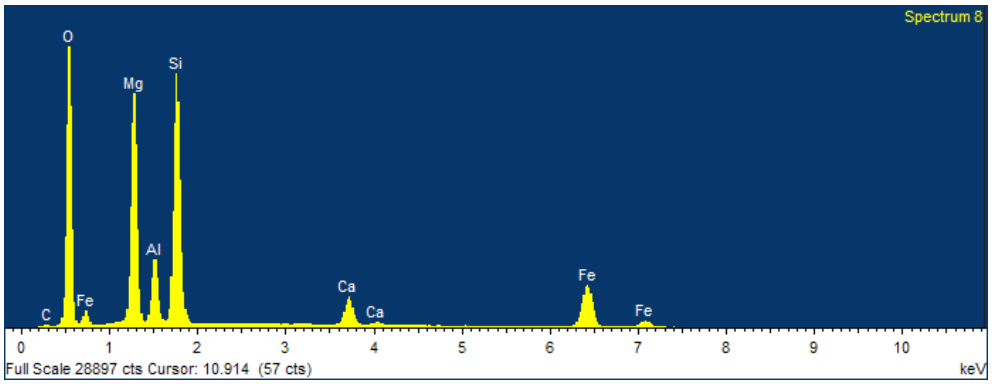

(b) Spectrum 8 of the mapping of NWA 11444 (ROI 1)

Figure A.31: X-Ray Spectra 7 and 8 of NWA 11444 (ROI 1)

Spectra 7 and 8 are located in regions in two different granules slightly brighter than the matrix but not as much as that of spectra 3 and 4. Specially for spectrum 7, the high peak of Mg suggests olivine. On the other hand, the equally high peak of Si and the presence of Al, Fe and Ca in similar intensities suggests a pyroxene, in this case, rich in Mg. Candidate minerals and their proportions are:

- Anorthite 23 %
- Clinoenstatite 6.1 %
- Fayalite 12.5 %

	Spectrum 7		Spectrum 8		Average	
Element	**Weight %**	**Atomic %**	**Weight %**	**Atomic %**	**Weight %**	**Atomic %**
C	1.54	2.65	1.62	2.82	1.58	2.735
O	47.57	61.66	47.61	62.22	47.59	61.94
Mg	17.89	15.26	15.45	13.28	16.67	14.27
Al	3.87	2.98	4.44	3.44	4.155	3.21
Si	17.11	12.63	16.97	12.63	17.04	12.63
Ca	2.46	1.27	2.68	1.4	2.57	1.335
Mn	0.17	0.06				
Fe	9.38	3.48	11.24	4.21	10.31	3.845
Totals	100	100	100	100		

Table A.23: Spectra 7 and 8 results for SEM/EDX microscopy of NWA 11444 (ROI 1)

- Fosterite 50.9 %
- Kamacite 4.7% (deprecated)
- Others <1%

This case is almost identical to Spectra 3 and 4, in which to distinguish between the two is necessary an additional analysis being with Raman Spectroscopy or with a polarised microscope.

ROI 2: Spectrum 1 and Spectrum 4

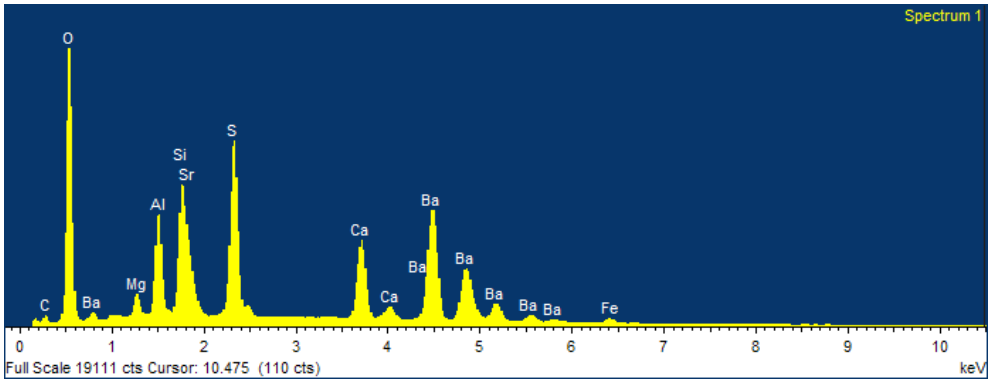

(a) Spectrum 1 of the mapping of NWA 11444, ROI 2

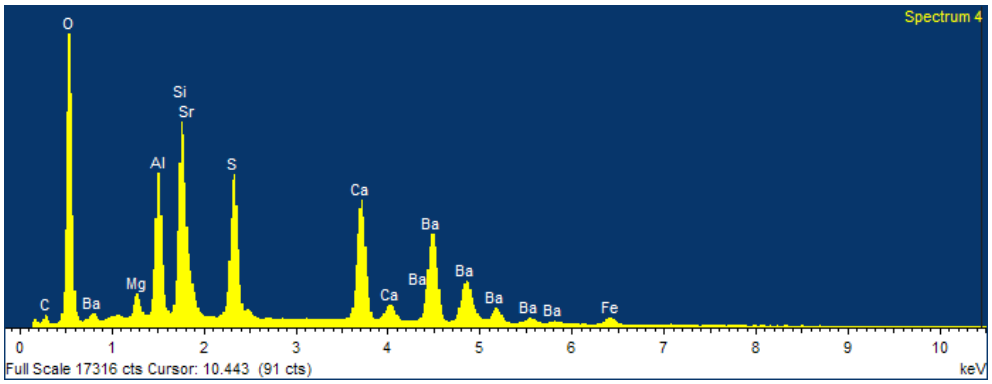

(b) Spectrum 4 of the mapping of NWA 11444, ROI 2

Figure A.32: X-Ray Spectra 1 and 4 of NWA 11444 (ROI 2)

	Spectrum 1		Spectrum 4		Average	
Element	**Weight %**	**Atomic %**	**Weight %**	**Atomic %**	**Weight %**	**Atomic %**
C	3.95	8.79	4.47	9.2	4.21	8.995
O	37.15	62.07	40.1	61.94	38.625	62.005
Mg	1.17	1.28	1.15	1.16	1.16	1.22
Al	4.61	4.56	6.09	5.58	5.35	5.07
Si	5.44	5.18	7.96	7	6.7	6.09
S	8.95	7.46	6.93	5.34	7.94	6.4
Ca	4.8	3.2	7.11	4.38	5.955	3.79
Fe	0.75	0.36	1.15	0.51	0.95	0.435
Sr	5.72	1.75	3.68	1.04	4.7	1.395
Ba	27.45	5.34	21.36	3.84	24.405	4.59
Totals	100	100	100	100		

Table A.24: Spectra 1 and 4 results for SEM/EDX microscopy of NWA 11444 (ROI 2)

Spectrum 1 and Spectrum 4 (ROI 2) are located inside a crack in the matrix meteorite. This fissure in the matrix is filled with a mineral (or minerals) that appear as bright white

in the SEM/EDX analysis. These minerals are abundant in Si, Al, Ca, S, Sr (strontium) and Ba (barium). Unfortunately, for this case MINSQ cannot converge as neither Sr nor Ba are included in any of the possible mineral compositions. This spectrum needs further analysis with Raman Spectroscopy.

ROI 2: Spectrum 2

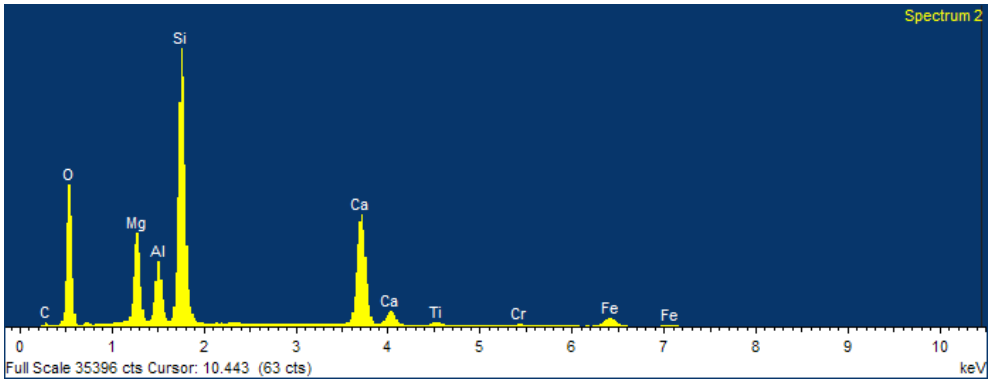

Figure A.33: X-Ray Spectrum 2 of NWA 11444 (ROI 2)

Spectrum 2 is located in a granule contained in the matrix. This granule is slightly brighter than the matrix and fractured in 3 different parts. Observing the peaks of Mg, Al, Si and Ca (as well as the small peak of Fe), one may conclude it is an augite with intermediate levels of Mg. The candidate minerals are:

- Albite 4.8 %
- Augite 82.6 %
- Labradorite 8.9 %
- Clinoenstatite 3.7 %
- Kamacite 1.9% (deprecated)

Element	Weight %	Atomic %
C	2.50	4.32
O	48.02	62.37
Mg	7.19	6.14
Al	4.54	3.50
Si	20.77	15.37
Ca	13.21	6.85
Ti	0.55	0.24
Cr	0.34	0.14
Fe	2.88	1.07
Totals	100.00	100.00

Table A.25: Spectrum 2 results for SEM/EDX microscopy of NWA 11444 (ROI 2)

ROI 2: Spectrum 3

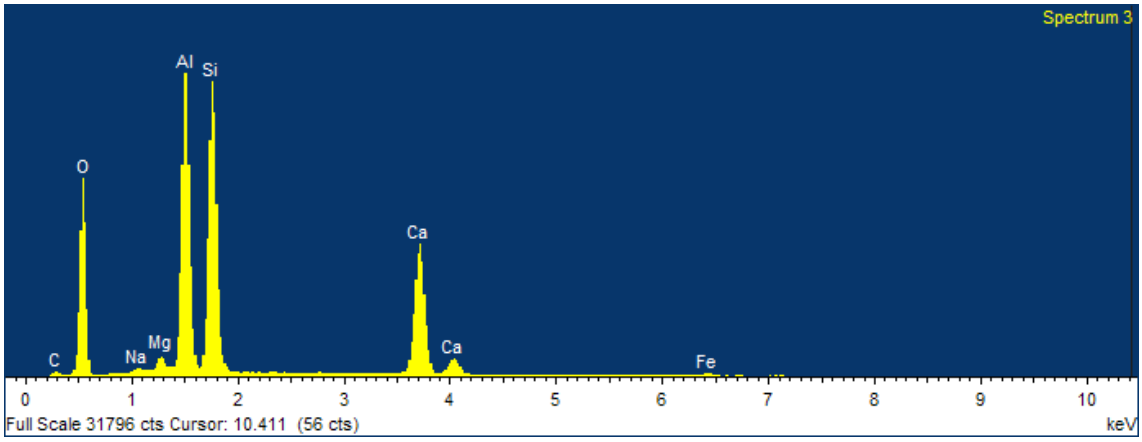

Figure A.34: X-Ray Spectrum 3 of NWA 11444 (ROI 2)

Element	Weight %	Atomic %
C	3.01	5.07
O	50.14	63.43
Na	0.24	0.21
Mg	0.76	0.63
Al	15.33	11.50
Si	17.82	12.84
Ca	12.09	6.10
Fe	0.63	0.23
Totals	100.00	100.00

Table A.26: Spectrum 3 results for SEM/EDX microscopy of NWA 11444 (ROI 2)

Spectrum 3 points directly in the matrix of the meteorite, a region of a greyish homogeneous colour. By observing the X-Ray peaks it is highly probably that the main mineral is plagioclase anorthite. The *twin* peaks of Al and Si along the peak of Ca at half of their intensity hint this mineral. Candidate minerals are:

- Anorthite 89.5 %
- Augite 9.5 %
- Others < 1 %

ROI 2: Spectrum 5

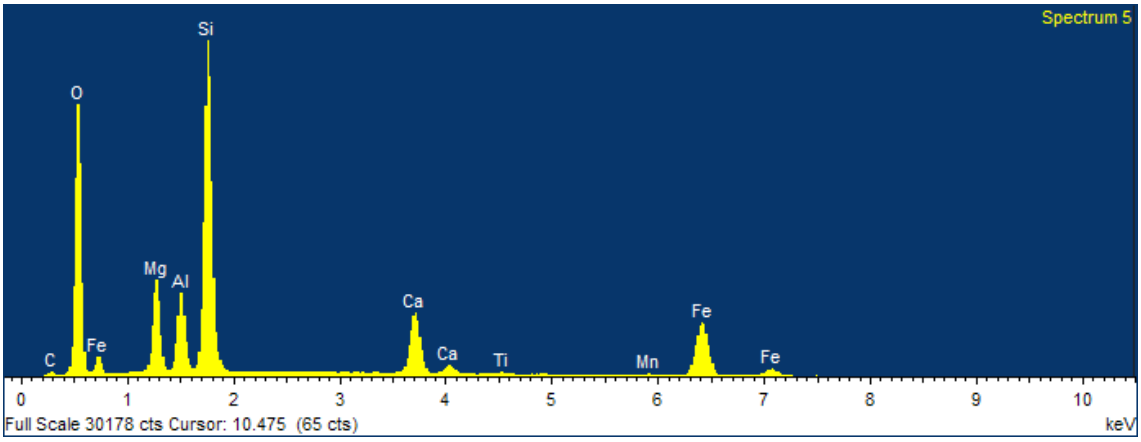

Figure A.35: X-Ray Spectrum 5 of NWA 11444 (ROI 2)

Spectrum 5 is located inside a granule of lighter grey colour, with several cracks inside. The spectrum obtained leads to different interpretations of the main mineral as the peaks of Ca and Fe alongside the Si peak and low Mg and Al suggest augite. However, a similar peak distribution can be obtained from an orthopyroxene (intermediate Mg and Fe) and anorthite (with the presence of the Al and the Ca peaks). The obtained minerals with their estimations are:

Element	Weight %	Atomic %
C	2.71	4.75
O	48.77	64.20
Mg	5.95	5.15
Al	4.55	3.55
Si	19.30	14.48
Ca	5.33	2.80
Ti	0.22	0.10
Mn	0.22	0.08
Fe	12.95	4.88
Totals	100.00	100.00

Table A.27: Spectrum 5 results for SEM/EDX microscopy of NWA 11444 (ROI 2)

- Anorthite 6.6 %
- Augite 20.7 %
- Pigeonite 37.9%
- Clinoenstatite 10.8%
- Ferrosilite 7.1 %
- Labradorite 23.1 %
- Kamacite 7.2 % (deprecated)
- Others < 1 %

There seems to be no primary mineral in this analysis. This sample should be further analysed with Raman Spectroscopy to be certain of the different minerals present.

ROI 3: Spectrum 1 and Spectrum 2

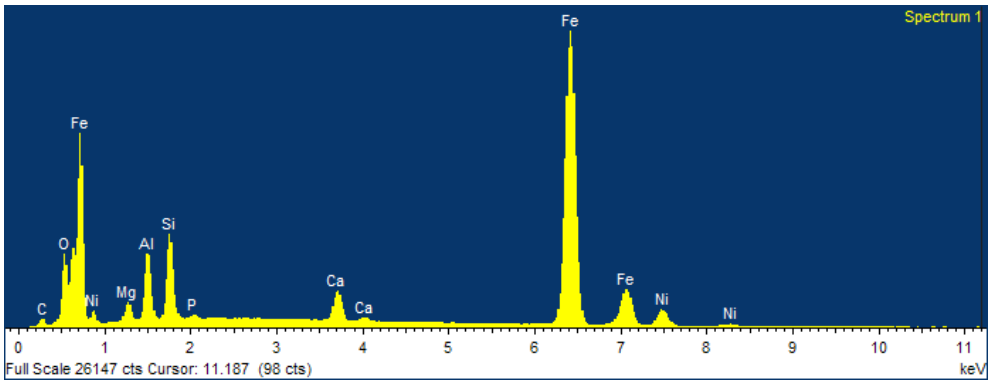

(a) [Spectrum 1 of the mapping of NWA 11444 (ROI 3)

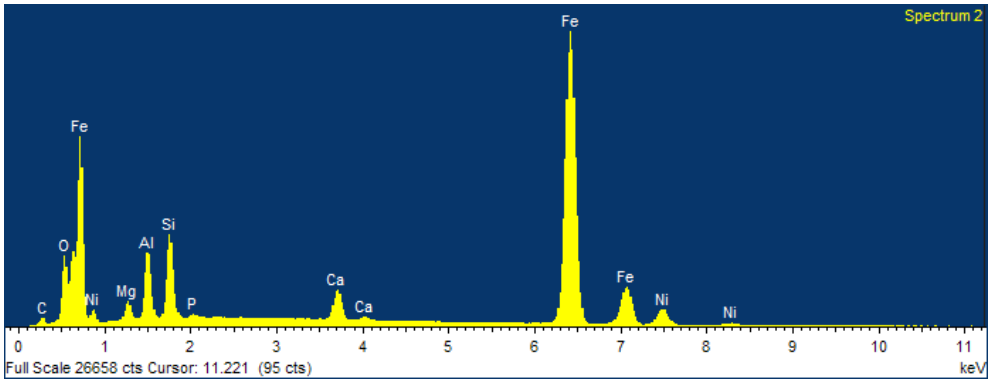

(b) Spectrum 2 of the mapping of NWA 11444 (ROI 3)

Figure A.36: X-Ray Spectra 1 and 3 of NWA 11444 (ROI 3)

	Spectrum 1		Spectrum 2		Average	
Element	**Weight %**	**Atomic %**	**Weight %**	**Atomic %**	**Weight %**	**Atomic %**
C	3.86	11.75	4.06	12.35	3.96	12.05
O	9.67	22.1	9.47	21.64	9.57	21.87
Mg	1.9	2.85	1.81	2.72	1.855	2.785
Al	5.07	6.87	5.14	6.96	5.105	6.915
Si	5.98	7.78	5.94	7.73	5.96	7.755
P	0.3	0.36	0.26	0.31	0.28	0.335
Ca	2.36	2.15	2.34	2.13	2.35	2.14
Fe	62.4	40.86	62.29	40.76	62.345	40.81
Ni	8.48	5.28	8.69	5.41	8.585	5.345
Totals	100	100	100	100		

Table A.28: Spectra 1 and 2 results for SEM/EDX microscopy of NWA 11444 (ROI 3)

Spectra 1 and 2 are located in a large granule of a bright colour white. Based on the X-Ray results, the grain is an iron grain. The first peak of Fe (at 0.7 keV) is the one indicating iron while the other (largest) indicates the presence of other minerals containing

Fe. For this particular case, MINSQ does not converge as none of the mineral components of the list has solely Fe. Qualitatively, taking into account the peaks in Si and O it is probable that a secondary mineral is fayalite.

ROI 3: Spectrum 3

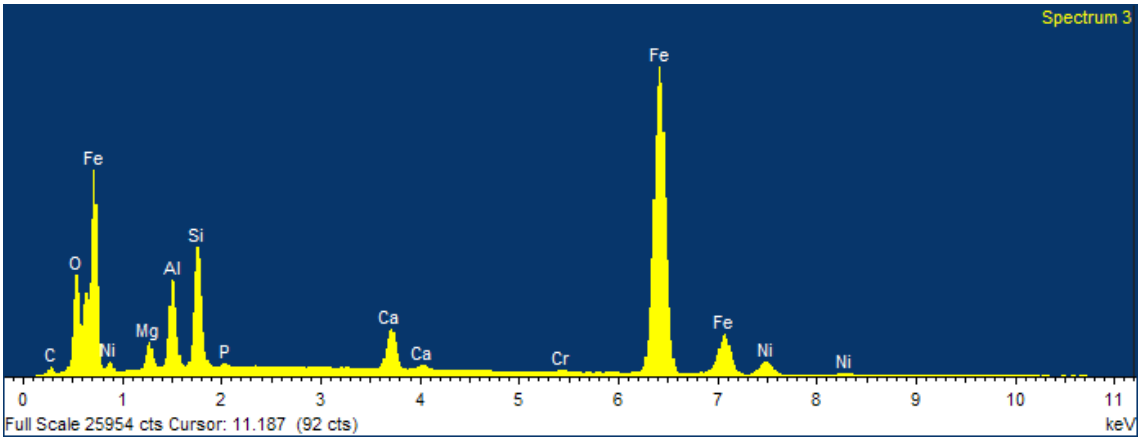

Figure A.37: X-Ray Spectrum 3 of NWA 11444, ROI B10-C10

Spectrum 3 is located in the border between the matrix and one of the white granules. Its X-Ray distribution is really similar to those of Spectra 1 and 2.

As in the previous case, only qualitative conclusions can be extracted: a grain of iron with fayalite. The rest of elements hint other minerals but need to be analysed with Raman Spectroscopy to verify their presence. For example, the small peaks of Ni could suggest the presence of kamacite. The combination of Al, Si and Ca could be from anorthite (in the border between the granule and the matrix).

Element	Weight %	Atomic %
C	3.74	10.71
O	12.53	26.96
Mg	2.24	3.17
Al	5.82	7.42
Si	7.33	8.98
P	0.24	0.27
Ca	2.90	2.49
Cr	0.19	0.13
Fe	58.42	36.01
Ni	6.59	3.86
Totals	100.00	100.00

Table A.29: Spectrum 3 results for SEM/EDX microscopy of NWA 11444 (ROI 3)

ROI 3: Spectrum 4 and Spectrum 5

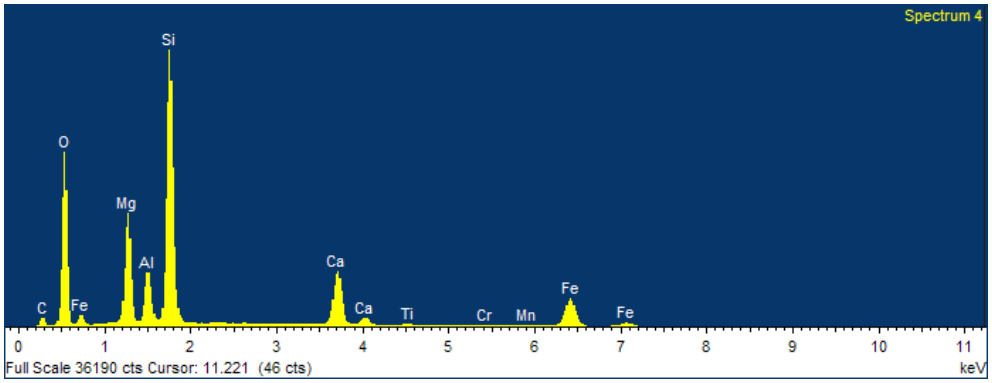

(a) Spectrum 4 of the mapping of NWA 11444 (ROI 3)

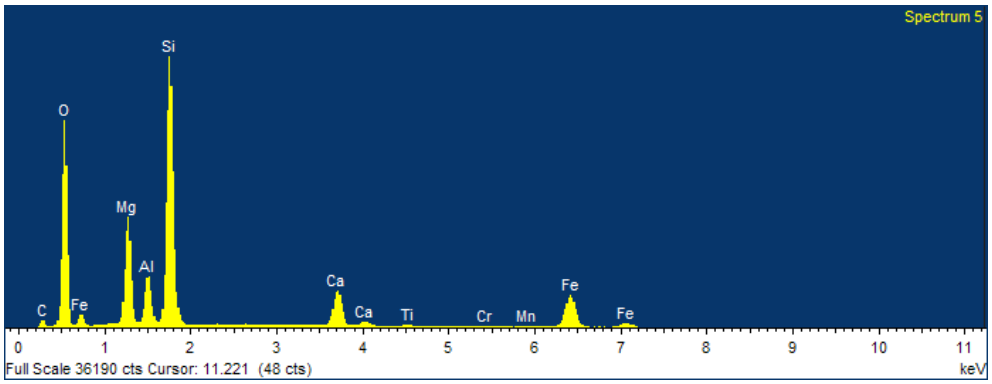

(b) Spectrum 5 of the mapping of NWA 11444 (ROI 3)

Figure A.38: X-Ray Spectra 4 and 5 of NWA 11444 (ROI 3)

	Spectrum 4		Spectrum 5		Average	
Element	**Weight %**	**Atomic %**	**Weight %**	**Atomic %**	**Weight %**	**Atomic %**
C	7.07	11.85	C	5.52	7.07	8.685
O	45.98	57.88	O	48.25	45.98	53.065
Mg	8.45	7	Mg	8.58	8.45	7.79
Al	3.64	2.72	Al	3.47	3.64	3.095
Si	19.93	14.29	Si	19.75	19.93	17.02
Ca	6.02	3.02	Ca	3.99	6.02	3.505
Ti	0.23	0.1	Ti	0.19	0.23	0.145
Cr	0.11	0.04	Cr	0.18	0.11	0.11
Mn	0.2	0.07	Mn	0.2	0.2	0.135
Fe	8.38	3.02	Fe	9.87	8.38	6.445
Totals	100	100	100	100		

Table A.30: Spectra 4 and 5 results for SEM/EDX microscopy of NWA 11444 (ROI 3)

Spectra 4 and 5 are located in a granule of almost unnoticeable lighter colour than the matrix. The results obtained in this region are similar to those obtained in Spectrum 5 for

ROI 2, with the difference that there is an additional element (in a marginal percentage): Cr. Hence, results are similar to those of Spectrum 5 of ROI 2:

- Anorthite 14.2 %
- Augite 23.4 %
- Pigeonite 41.8%
- Ferrosilite 11.2 %
- Fayalite 8.2 %
- Others $< 1\%$

ROI 3: Spectrum 6 and Spectrum 7

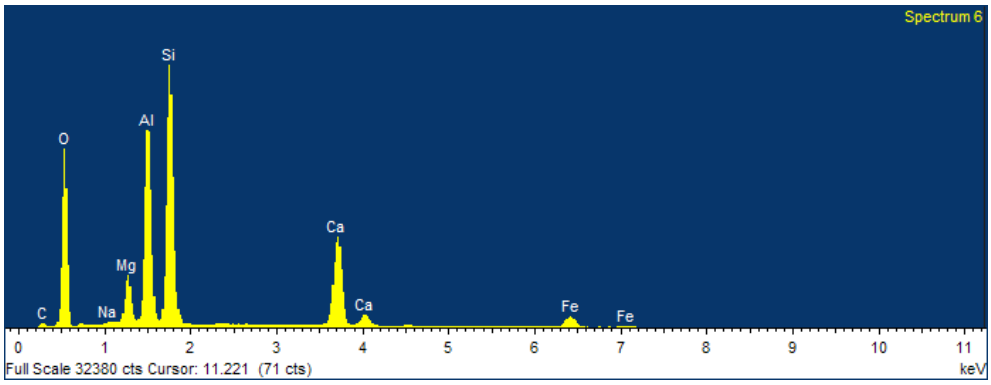

(a) Spectrum 6 of the mapping of NWA 11444 (ROI 3)

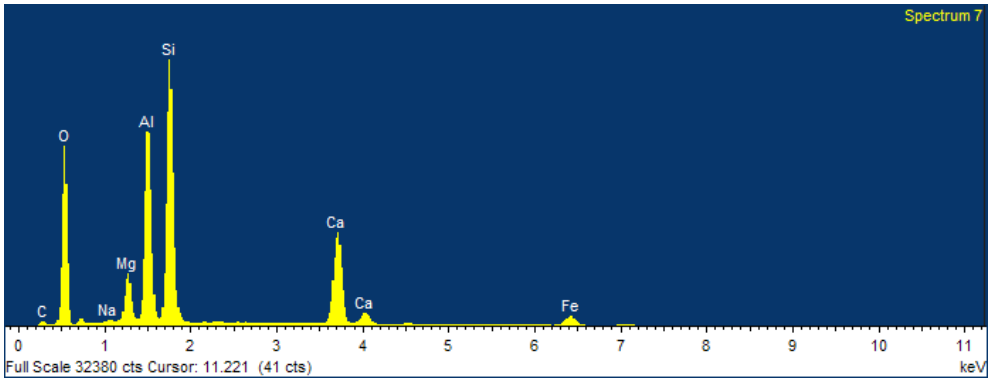

(b) Spectrum 7 of the mapping of NWA 11444 (ROI 3)

Figure A.39: Spectra 6 and 7 of the mapping of NWA 11444 (ROI 3)

	Spectrum 6		Spectrum 7		Average	
Element	**Weight %**	**Atomic %**	**Weight %**	**Atomic %**	**Weight %**	**Atomic %**
C	3.2	5.43	3.37	5.69	3.285	5.56
O	49.18	62.55	49.57	62.72	49.375	62.635
Na	0.21	0.18	0.24	0.21	0.225	0.195
Mg	3.36	2.81	3.36	2.8	3.36	2.805
Al	12.4	9.36	12.02	9.02	12.21	9.19
Si	18.7	13.55	18.82	13.56	18.76	13.555
Ca	9.78	4.96	9.94	5.02	9.86	4.99
Fe	3.17	1.15	2.67	0.97	2.92	1.06
Totals	100	100	100	100		

Table A.31: Spectra 6 and 7 results for SEM/EDX microscopy of NWA 11444 (ROI 3)

Spectra 6 and 7 are taken from the matrix of the meteorite. By the distribution of X-Ray peaks it is clear that the dominant mineral is plagioclase anorthite (prominent peaks of Al and Si and one of Ca with half of their intensity). Secondary peaks of Mg, Na and Fe can come from either pyroxenes or olivines. The candidate minerals are:

- Anorthite 69.6%
- Augite 5.4%
- Pigeonite 21.6%
- Labradorite 3.1%

As the X-Ray analysis is a preliminary study to determine the minerals in the sample, for Spectra 6 and 7 the principal mineral is considered to be anorthite. As secondary minerals and pending to be verified by other independent means are considered to be pigeonite and marginally augite and labradorite.

ROI 3: Spectrum 8

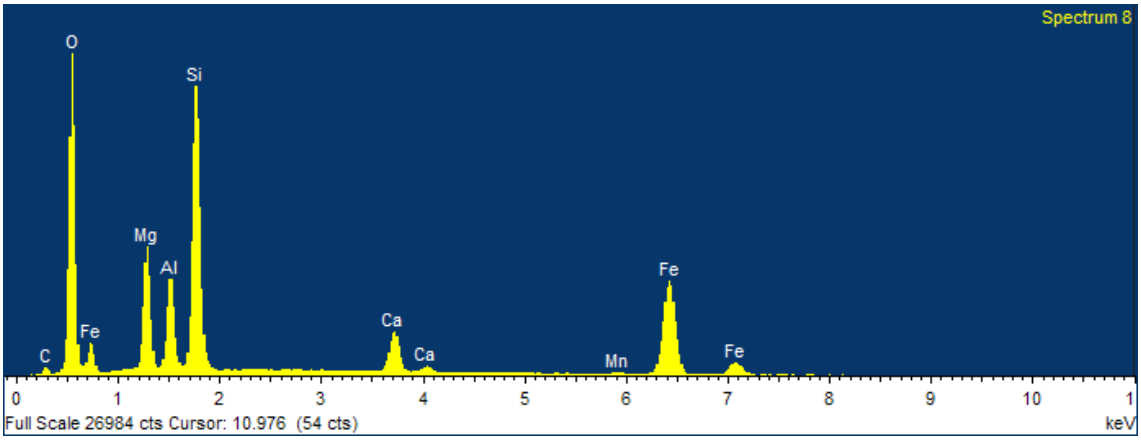

Figure A.40: X-Ray Spectrum 8 of NWA 11444 (ROI 3)

Element	Weight %	Atomic %
C	3.98	7.16
O	45.11	60.98
Mg	7.51	6.68
Al	4.94	3.96
Si	15.25	11.75
Ca	3.18	1.72
Mn	0.23	0.09
Fe	19.80	7.67
Totals	100.00	100.00

Table A.32: Spectrum 8 results for SEM/EDX microscopy of NWA 11444 (ROI 3)

Spectrum 8 is also on a lighter grey grain, hardly defined, blurred in the matrix. The spectrum is similar to those obtained in the region of Spectrum 4 and 5 but with the difference that there is no Ti nor Cr. The mineral candidates are:

- Anorhite 28.1%
- Clinoenstatite 12.5%
- Ferrosilite 10.3%
- Fayalite 20.6%
- Olivine 17.2%
- Labradorite 2.3%
- Kamacite 9 % (deprecated)
- Others < 1 %

ROI 3: Spectrum 9

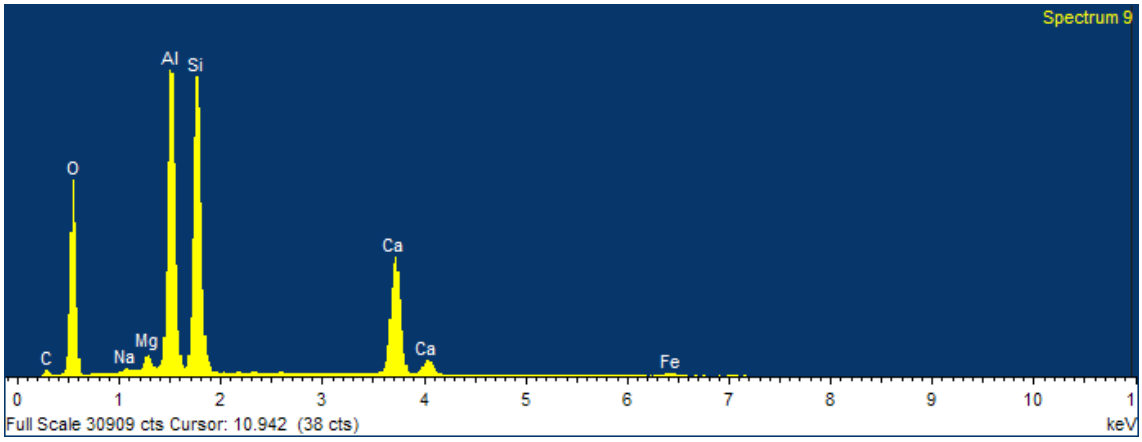

Figure A.41: X-Ray Spectrum 9 of NWA 11444 (ROI 3)

Spectrum 9 belongs to the matrix, from a region that it looks totally homogeneous and smooth (with no granules, cracks or other imperfections). The X-Ray obtained is clearly an anorthite displaying the *twin peak* of Al and Si and the secondary peak of Ca. Results are:

- Anorthite 92.4%
- Fayalite 1.2%
- Olivine Fosterite 2.5%
- Labradorite 3.9%
- Others $< 1\%$

Element	**Weight %**	**Atomic %**
C	3.96	6.62
O	49.44	62.09
Na	0.29	0.25
Mg	0.80	0.66
Al	15.46	11.52
Si	18.23	13.04
Ca	11.12	5.58
Fe	0.70	0.25
Totals	100.00	100.00

Table A.33: Spectrum 9 results for SEM/EDX microscopy of NWA 11444 (ROI 3)

Mapping

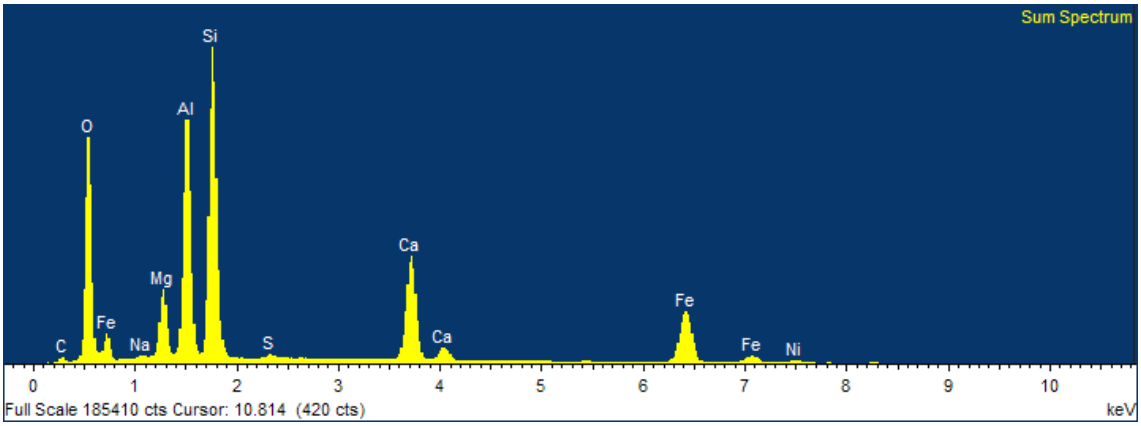

Figure A.42: X-Ray Spectrum of NWA 11444 mapping, magnified ROI B10-C10 (ROI 4), for the mapping

The most important feature of this mapping is the iron grain. In Figure 3.15 can be observed that the white area enclosed from the matrix is exclusively from Fe. Particularly, the lower right edge concentrates all the S of the sample which along the Fe could be forming iron sulphide or a rarer mineral, troilite. Also, the concentration of Ni is found in the same region of the iron grain, meaning that the grain is not purely of iron but a Ni-Fe mineral is found (kamacite). Much fainter, the quantities of Cr and P seem also to be higher in the grain region. In contrast, it is intuitively to distinguish the anorthite matrix: the brightness of Al and Si is very similar and homogeneous while the one for Ca is also evenly distributed but of lower intensity. Eventually, if comparing 3.15.b with 3.15.c the regions with most Mg are the ones that display the lowest concentrations of Al and low in Ca. Those probably indicate the presence of orthopyroxenes.

Element	**Weight %**	**Atomic %**
C	3.74	6.72
O	42.95	57.93
Na	0.20	0.19
Mg	3.78	3.35
Al	11.89	9.51
Si	17.06	13.11
S	0.23	0.15
Ca	8.32	4.48
Fe	11.12	4.30
Ni	0.71	0.26
Totals	100.00	100.00

Table A.34: Spectrum of the mapping for SEM/EDX microscopy of NWA 11444 (ROI 4)

For this particular case, the values of the weight and atomic percentages are not as relevant as the iron grain becomes averaged by the rest of the matrix, obtaining a 60% in weight composition of anorthite mineral.